Two-loop renormalization-group theory for the quasi-one-dimensional Hubbard model at half filling

M. Tsuchiizu
Department of Physics, Nagoya University, Nagoya 464-8602, Japan
(Dated: February 6, 2008)

We derive two-loop renormalization-group equations for the half-filled one-dimensional Hubbard chains coupled by the interchain hopping. Our renormalization-group scheme for the quasi-one-dimensional electron system is a natural extension of that for the purely one-dimensional systems in the sense that transverse-momentum dependences are introduced in the g-ological coupling constants and we regard the transverse momentum as a patch index. We develop symmetry arguments for the particle-hole symmetric half-filled Hubbard model and obtain constraints on the g-ological coupling constants by which resultant renormalization equations are given in a compact form. By solving the renormalization-group equations numerically, we estimate the magnitude of excitation gaps and clarify that the charge gap is suppressed due to the interchain hopping but is always finite even for the relevant interchain hopping. To show the validity of the present analysis, we also apply this to the two-leg ladder system. By utilizing the field-theoretical bosonization and fermionization method, we derive low-energy effective theory and analyze the magnitude of all the excitation gaps in detail. It is shown that the low-energy excitations in the two-leg Hubbard ladder have SO(3)×SO(3)×U(1) symmetry when the interchain hopping exceeds the magnitude of the charge gap.

PACS numbers: 71.10.Fd, 71.10.Hf, 71.10.Pm

I. INTRODUCTION

Renormalization-group (RG) method is one of the most powerful and promising tools to tackle low-dimensional electron and spin systems.[1] It has a long history of research especially on one dimensional (1D) systems, since the RG theory is superior to take into account low-dimensional competing fluctuation effects, i.e., it can sum up systematically the logarithmic-singular particle-particle and particle-hole channels which appear in all order of perturbation theory.[2,3,4] It has been clarified that the RG method describes various 1D ground states: the Tomonaga-Luttinger (TL) liquid state, the charge-gapped Mott insulating state at half filling, and also the spin-gapped Luther-Emery state.[1,5] Not only for the most divergent terms, the next-to-leading logarithmic singular terms have also been studied based on the two-loop formulation of the RG theory,[3,4] where singular self-energy corrections in addition to the vertex corrections are taken into account. Recently the RG theory is generalized to apply to two-dimensional electron systems.[6] The main difficulty in the RG formulation for two-dimensional systems resides in the fact that the momentum dependence of the coupling constants is essential but the number of independent coupling constants is large and it becomes hard to analyze the RG equations even for the one-loop level. Several attempts have been made by focusing only on dominant scattering processes on the Fermi surface[7] and by discretizing the Fermi surface into finite number of pieces, i.e., so-called patches.[8] For electron systems in arbitrary dimension, a nonperturbative RG theory has also been formulated[9] and has been applied to two dimensional electron systems by considering leading two particle interactions, i.e., within the one-loop level.[10,11] Quite recently the effect of the two-loop self-energy corrections have been examined,[12,13,14,15] while the two-loop vertex corrections are considered only for the system with flat Fermi surface.[16,17]

In quasi-one-dimensional (Q1D) electron systems, the important issue to be clarified is the dimensional crossover from one to higher dimensions which would occur by changing parameters or temperature.[1,5,18] In real Q1D compounds, the TL-liquid behavior is expected at high temperature, however, the effect of warping of the Fermi surface due to the small but finite interchain hopping is enhanced at low temperature where the Fermi-liquid behavior can be expected if the system is metallic, and finally the system has an instability to symmetry-broken states. The RG approach is also powerful and succeeds in the description of these physical pictures.[1,4,5,19] In the early RG analysis, the effect of the one-particle interchain hopping is treated perturbatively, however, it is found to be relevant even in the noninteracting case and the perturbative treatment is invalid at low temperature. In order to clarify the dimensional crossover phenomena properly, one has to formulate the RG with the nonperturbative treatment of the interchain hopping, i.e., based on the warped Fermi surface. In this sense, the formulation is analogous to that in the two-dimensional RG scheme since one has to discretize the Fermi surface. In the Q1D case, the RG has been formulated by considering finite number of chains $N_\perp$ ($N_\perp$-chain RG scheme)[20,21,22,23,24,25,26] where the transverse momentum is regarded as a patch index. Based on this scheme, the Q1D systems have been analyzed intensively within the one-loop level[20,21,22,23,24,25] and the self-energy corrections have also been investigated.[26] At commensurate band filling, the dimensional crossover problem becomes nontrivial since the electronic correlation has the strongest effect and leads to the Mott insulating state if the system is half filled. The effect of the umklapp scattering between electrons, which is a trigger for the 1D Mott insulator, has been investigated by the one-loop RG,[22] however, in order to clarify the electronic states in the Mott insulator one has to examine the properties of the one-particle Green's function, i.e., the self-energy corrections, whose singular contributions only appear beyond the one-loop level. The effects of the two-loop self-energy corrections have also been examined in the Q1D systems without considering two-loop vertex corrections,[26] however, a systematic two-loop RG including

both the two-loop vertex and self-energy corrections is not formulated yet. Recently this issue has also been addressed by a numerical method expanding the dynamical mean-field approach (chain-DMFT)[27,28,29,30] and by a field-theoretical method with the RPA treatment of the interchain hopping.[31]

From a technical point of view, it is generally hard to gain physical insights of results of scaling flows in the Q1D RG, since the number of independent coupling constants becomes large as $N_\perp$ increases. As a minimal system of the coupled chains, one can consider a two-leg ladder system ($N_\perp = 2$). The two-leg ladder system itself has nontrivial and interesting features[32] and has been examined intensively by using the RG method[33,34,35,36,37,38,39,40,41,42] and also by the high-accuracy numerical technique called the density-matrix-renormalization-group (DMRG) method,[43,44] where it has been confirmed that both the charge and spin modes have excitation gaps for the half-filled Hubbard ladder. In this analysis, one can easily see that a naive one-loop RG analysis of the excitation gaps is not satisfactory since the RG method breaks down at a energy scale corresponding to the largest excitation gap in a system. In order to analyze the lower-energy properties, one has to derive an effective theory by tracing out the gapped modes based on the field-theoretical bosonization/fermionization treatment. As for the two-leg Hubbard ladder, Lin, Balents and Fisher[38] obtained the SO(8) Gross-Neveu model as an effective theory in the low-energy limit and examined the excitation spectrum. The extended two-leg Hubbard model including additional interactions is also examined[40,41,42] and quantum phase transitions between competing ground states have been clarified in this context of the one-loop RG. Despite that the analysis of the two-leg ladder systems based on the one-loop RG succeeds in describing the ground state properties, it is not easy to extend the analysis to the case with large number of chains, since the field-theoretical approach is restricted to the small number of chains. In order to overcome this problem, we formulate, in the present paper, the two-loop RG theory for the Q1D electron systems. Even in the two-loop level, the perturbative approach also breaks down at energy scales of the excitation gaps, however, the respective excitation gaps can be estimated by analyzing the scaling behavior of the couplings for respective modes, without following the tracing-out procedure. We confirm that the present scheme works even if the respective modes are not independent by revisiting the two-leg ladder systems.

This paper is organized as follows. In Sec. II, we introduce the finite $N_\perp$-chain half-filled Hubbard model coupled by the one-particle interchain hopping, and derive the corresponding g-ology model by linearizing the energy dispersion where the effect of the interchain hopping is treated nonperturbatively. By developing symmetry arguments for the particle-hole symmetric half-filled Hubbard model, we obtain constraints on the g-ological coupling constants. In Sec. III, we formulate the RG based on the Kadanoff-Wilson approach up to the two-loop level, where vertex corrections are taken into account based on the third-order perturbation theory, in addition to the second-order calculation for the self-energy corrections. Reflecting the symmetries that the particle-hole symmetric Hubbard model has, the resultant RG equations can be written in a compact form where the physical picture can easily be captured. By solving the RG equations numerically, we estimate the magnitude of the charge and spin gaps. In Sec. IV, in order to indicate the validity of the present method, we consider a most simple but nontrivial case $N_\perp = 2$, which corresponds to the two-leg ladder, and analyze the excitation properties in detail by combining the field-theoretical bosonization and fermionization method. Finally, the results are summarized in Sec. V. Technical details are given in the Appendices A and B. In the Appendix C, we give a related issue which supports strongly the validity of the present estimation of excitation gaps.

II. MODEL AND SYMMETRY ARGUMENTS

We consider the bipartite Q1D Hubbard model at half filling with $t_\parallel \gg t_\perp$, where the transfer integral along chains is $t_\parallel$ and that between chains is $t_\perp$. Our Hamiltonian is given by

$$\begin{aligned} H &= -t_\parallel \sum_{j,l,s} \left(c^\dagger_{j,l,s} c_{j+1,l,s} + \text{H.c.} \right) \\ &\quad - t_\perp \sum_{j,l,s} \left(c^\dagger_{j,l,s} c_{j,l+1,s} + \text{H.c.} \right) \\ &\quad + U \sum_{j,l} n_{j,l,\uparrow} n_{j,l,\downarrow}, \end{aligned} \tag{2.1}$$

where $c_{j,l,s}$ is the annihilation operator of electron on the jth site in the lth chain with spin s, and $n_{j,l,s} = c^\dagger_{j,l,s} c_{j,l,s} - \frac{1}{2}$. The system size along chains ($N_\parallel$) is considered to be sufficiently large and the sum of the site index, which runs $j = 1, \cdots, N_\parallel$, is to be understood as an integral in the thermodynamic limit. The chain index runs $l = 1, \cdots, N_\perp$ and we consider the system with finite number of chains $N_\perp$ where the periodic boundary condition is imposed $c_{j,N_\perp+1,s} = c_{j,1,s}$.

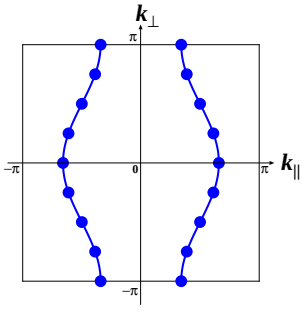

FIG. 1: (Color online) Fermi points (closed circles) in the present half-filled Q1D Hubbard model with the periodic boundary condition in the transverse direction. The case for $N_\perp = 8$ is shown.

A. g-ology notation

The kinetic term of the Hamiltonian is given by

$$H_0 = \sum_{\boldsymbol{k},s} \varepsilon(\boldsymbol{k})\, c_s^\dagger(\boldsymbol{k})\, c_s(\boldsymbol{k}), \tag{2.2}$$

$$\varepsilon(\boldsymbol{k}) = -2t_\parallel \cos k_\parallel - 2t_\perp \cos k_\perp, \tag{2.3}$$

where $\boldsymbol{k} = (k_\parallel, k_\perp)$ and the lattice constant is set to unity. Since the system is particle-hole symmetric, we can assume $t_\parallel > 0$ and $t_\perp \geq 0$ without losing generality. Since the number of chains $N_\perp$ is finite, the transverse momentum is given by

$$k_\perp = \frac{2\pi}{N_\perp} n, \quad n = -\left[\frac{N_\perp}{2}\right], ..., \left[\frac{N_\perp}{2}\right], \tag{2.4}$$

where $[x]$ is the Gauss symbol denoting maximum integer which does not exceed x. By assuming $t_\perp \ll t_\parallel$, we linearize the dispersion where the situation can be simplified as follows. Up to the lowest order in $t_\perp$ the kinetic term with the linearized dispersion is given by

$$H_0 = \sum_{\boldsymbol{k},p,s} \varepsilon_p(\boldsymbol{k})\, c_{p,s}^\dagger(\boldsymbol{k})\, c_{p,s}(\boldsymbol{k}), \tag{2.5}$$

$$\varepsilon_p(\boldsymbol{k}) = v(pk_\parallel - k_F) - 2t_\perp \cos k_\perp, \tag{2.6}$$

where $v = 2t_\parallel$ and $k_F = \pi/2$. We introduce the bandwidth cutoff Λ. In this approximation, the warped open Fermi surface (Fig. 1) is specified as a function of $k_\perp$:

$$k_F(k_\perp) = k_F + 2\frac{t_\perp}{v}\cos k_\perp, \tag{2.7}$$

and the energy dispersion (2.6) can be reexpressed as $\varepsilon_p(\boldsymbol{k}) = v[pk_\parallel - k_F(k_\perp)]$. Thus we regard the transverse momentum $k_\perp$ as a *patch index* in the present RG formulation. The greatest merit of the present formulation lies in the fact that the transverse momentum $k_\perp$ is a conserved quantity, i.e., the patch index is a good quantum number and the ambiguity of selecting patch index disappears.

Following the conventional g-ology approach,[3] we classify the interaction part of the Hamiltonian $H_{\rm I} = U\sum_{j,l} n_{j,l,\uparrow} n_{j,l,\downarrow}$ into the forward, backward, and umklapp scattering processes, by focusing on the longitudinal momentum $k_\parallel$. We introduce the coupling constants $g_{1\perp}$, $g_{2\perp}$, $g_\parallel$, $g_{3\perp}$, and $g_{3\parallel}$, which represent the backward scattering with the opposite spins ($g_{1\perp}$), the forward scattering with the opposite spins ($g_{2\perp}$), the forward scattering with the same spins ($g_\parallel$), the umklapp scattering with the opposite spins ($g_{3\perp}$), and the umklapp scattering with the same spins ($g_{3\parallel}$). In terms of the Hubbard interaction U, the magnitudes of the couplings are given by $g_{1\perp} = g_{2\perp} = g_{3\perp} = U$ and $g_\parallel = g_{3\parallel} = 0$. The $g_\parallel$ and $g_{3\parallel}$ processes are absent in the original Hubbard interactions, however, can become finite under the RG scaling procedure. Furthermore, the coupling constants are differently renormalized depending on the external transverse momenta of the vertex and have the explicit transverse-momentum (i.e., patch-index) dependence. To take into account these effects, we formally introduce the transverse momentum dependence of the coupling constants in the initial g-ology Hamiltonian. In the most general form, the interaction part of the Hamiltonian is given by

$$\begin{aligned}
H_{\rm I} = {} & +\frac{1}{V}\sum_{\boldsymbol{k}_1,\boldsymbol{k}_2,\boldsymbol{q},s} g_{1\perp(q_\perp,k_{\perp 1},k_{\perp 2})}\; c_{+,s}^\dagger(\boldsymbol{k}_1)\, c_{-,s}(\boldsymbol{k}_1-\boldsymbol{Q})\; c_{-,\bar{s}}^\dagger(\boldsymbol{k}_2-\boldsymbol{Q})\, c_{+,\bar{s}}(\boldsymbol{k}_2) \\
& + \frac{1}{V}\sum_{\boldsymbol{k}_1,\boldsymbol{k}_2,\boldsymbol{q},s} g_{2\perp(q_\perp,k_{\perp 1},k_{\perp 2})}\; c_{+,s}^\dagger(\boldsymbol{k}_1)\, c_{+,s}(\boldsymbol{k}_2)\; c_{-,\bar{s}}^\dagger(\boldsymbol{k}_2-\boldsymbol{Q})\, c_{-,\bar{s}}(\boldsymbol{k}_1-\boldsymbol{Q}) \\
& + \frac{1}{V}\sum_{\boldsymbol{k}_1,\boldsymbol{k}_2,\boldsymbol{q},s} g_{\parallel(q_\perp,k_{\perp 1},k_{\perp 2})}\; c_{+,s}^\dagger(\boldsymbol{k}_1)\, c_{+,s}(\boldsymbol{k}_2)\; c_{-,s}^\dagger(\boldsymbol{k}_2-\boldsymbol{Q})\, c_{-,s}(\boldsymbol{k}_1-\boldsymbol{Q}) \\
& + \frac{1}{2V}\sum_{\boldsymbol{k}_1,\boldsymbol{k}_2,\boldsymbol{q},s} g_{3\perp(q_\perp,k_{\perp 1},k_{\perp 2})}\Big[c_{+,s}^\dagger(\boldsymbol{k}_1)\, c_{-,s}(\boldsymbol{k}_1-\boldsymbol{Q})\; c_{+,\bar{s}}^\dagger(\boldsymbol{k}_2)\, c_{-,\bar{s}}(\boldsymbol{k}_2+\boldsymbol{Q}-\boldsymbol{G}) + \text{H.c.}\Big] \\
& + \frac{1}{2V}\sum_{\boldsymbol{k}_1,\boldsymbol{k}_2,\boldsymbol{q},s} g_{3\parallel(q_\perp,k_{\perp 1},k_{\perp 2})}\Big[c_{+,s}^\dagger(\boldsymbol{k}_1)\, c_{-,s}(\boldsymbol{k}_1-\boldsymbol{Q})\; c_{+,s}^\dagger(\boldsymbol{k}_2)\, c_{-,s}(\boldsymbol{k}_2+\boldsymbol{Q}-\boldsymbol{G}) + \text{H.c.}\Big],
\end{aligned} \tag{2.8}$$

where $\bar{s} = \uparrow(\downarrow)$ for $s = \downarrow(\uparrow)$, and $\boldsymbol{Q} = (\pi + q_\parallel, q_\perp)$, $\boldsymbol{G} = (2\pi, 0)$, and $V = N_\parallel N_\perp$. The momenta $k_{\parallel 1}$ and $k_{\parallel 2}$ are assumed to take values near $k_F(k_\perp)$. In the transverse direction, on the other hand, the momenta $k_{\perp i}$ and $q_\perp$ can take the values in $-\pi < k_{\perp i}, q_\perp \leq \pi$, and the momentum $(k_{\perp i} \pm q_\perp)$ is assumed to reduce the first Brillouin zone, then all the possible scattering processes are taken into account, including the transverse umklapp scattering. The respective scattering processes are shown in Fig. 2. We will neglect the forward scattering with the same branch, so-called g_4 term, since this

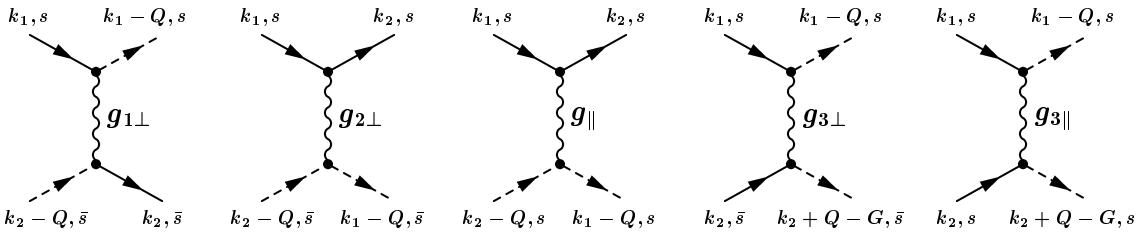

FIG. 2: g-ology notation. The solid (dashed) line denotes a right-moving (left-moving) electron. $\boldsymbol{k}_i = (k_{\parallel i}, k_{\perp i})$, $\boldsymbol{Q} = (\pi + q_\parallel, q_\perp)$, and $\boldsymbol{G} = (2\pi, 0)$.

process does not show the logarithmic-singular behavior in perturbation and is known to yield only quantitative changes in velocities for the 1D case. In terms of the Hubbard interaction U, the magnitudes of the couplings are given by $g_{1\perp(q_\perp,k_{\perp 1},k_{\perp 2})} = g_{2\perp(q_\perp,k_{\perp 1},k_{\perp 2})} = g_{3\perp(q_\perp,k_{\perp 1},k_{\perp 2})} = U$ and $g_{\parallel(q_\perp,k_{\perp 1},k_{\perp 2})} = g_{3\parallel(q_\perp,k_{\perp 1},k_{\perp 2})} = 0$. To simplify the notation, we will suppress the $\perp$ index of the transverse momentum in the following. All the coupling constants are assumed to be real. In order to make $H_{\rm I}$ hermitian, the coupling constants must satisfy

$$\begin{aligned} g_{1\perp(q,k_1,k_2)} &= g_{1\perp(q,k_2,k_1)}, \\ g_{2\perp(q,k_1,k_2)} &= g_{2\perp(q,k_2,k_1)}, \\ g_{\parallel(q,k_1,k_2)} &= g_{\parallel(q,k_2,k_1)}, \\ g_{3\perp(q,k_1,k_2)} &= g_{3\perp(-q,k_2,k_1)}, \\ g_{3\parallel(q,k_1,k_2)} &= g_{3\parallel(-q,k_2,k_1)}. \end{aligned} \tag{2.9}$$

As in the 1D case, the physical picture becomes transparent by introducing a new set of the couplings:

$$\begin{aligned} g_{\rho(q,k_1,k_2)} &\equiv g_{2\perp(q,k_1,k_2)} + g_{\parallel(q,k_1,k_2)}, \\ g_{\sigma(q,k_1,k_2)} &\equiv g_{2\perp(q,k_1,k_2)} - g_{\parallel(q,k_1,k_2)}, \\ g_{c(q,k_1,k_2)} &\equiv g_{3\perp(q,k_1,\pi-k_2)}, \\ g_{s(q,k_1,k_2)} &\equiv g_{1\perp(q,k_1,k_2)}, \\ g_{cs(q,k_1,k_2)} &\equiv g_{3\parallel(q,k_1,\pi-k_2)}, \end{aligned} \tag{2.10}$$

where g_ρ and g_c (g_σ and g_s) are the coupling constants representing the charge (spin) degrees of freedom. This picture can easily be captured by noting that, if we neglect the momentum dependence of the coupling constants, the $g_{1\perp}$, $g_{2\perp}$, $g_\parallel$, and $g_{3\perp}$ terms of the Hamiltonian (2.8) are written in symmetric forms as[45]

$$\begin{aligned} &-\frac{g_\sigma}{V}\sum_{p,\boldsymbol{q}} J^z_p(\boldsymbol{q}) J^z_{-p}(-\boldsymbol{q}) - \frac{g_s}{V}\sum_{p,\boldsymbol{q}} J^+_p(\boldsymbol{q}) J^-_{-p}(-\boldsymbol{q}) \\ &+\frac{g_\rho}{V}\sum_{p,\boldsymbol{q}} J'^z_p(\boldsymbol{q}) J'^z_{-p}(-\boldsymbol{q}) + \frac{g_c}{V}\sum_{p,\boldsymbol{q}} J'^+_p(\boldsymbol{q}) J'^-_{-p}(-\boldsymbol{q}), \end{aligned} \tag{2.11}$$

where the respective chiral density operators are given by

$$J^z_p(\boldsymbol{q}) = \frac{1}{2}\sum_{\boldsymbol{k},s}\Big[c^\dagger_{p,\uparrow}(\boldsymbol{k})\, c_{p,\uparrow}(\boldsymbol{k}+\boldsymbol{q}) - c^\dagger_{p,\downarrow}(\boldsymbol{k})\, c_{p,\downarrow}(\boldsymbol{k}+\boldsymbol{q})\Big], \tag{2.12a}$$

$$J'^z_p(\boldsymbol{q}) = \frac{1}{2}\sum_{\boldsymbol{k},s} :\, c^\dagger_{p,s}(\boldsymbol{k})\, c_{p,s}(\boldsymbol{k}+\boldsymbol{q}) :, \tag{2.12b}$$

$$J^-_p(\boldsymbol{q}) = \sum_{\boldsymbol{k}} c^\dagger_{p,\downarrow}(\boldsymbol{k})\, c_{p,\uparrow}(\boldsymbol{k}+\boldsymbol{q}), \tag{2.12c}$$

$$J'^-_p(\boldsymbol{q}) = \sum_{\boldsymbol{k}} c_{p,\uparrow}(\boldsymbol{k})\, c_{p,\downarrow}\big((\pi,\pi) - \boldsymbol{k} + \boldsymbol{q}\big), \tag{2.12d}$$

and $J^+_p(\boldsymbol{q}) = [J^-_p(-\boldsymbol{q})]^\dagger$, $J'^+_p(\boldsymbol{q}) = [J'^-_p(-\boldsymbol{q})]^\dagger$. In the 1D half-filled Hubbard model ($g_\rho = g_c$ and $g_\sigma = g_s$), it is known that the charge part, in addition to the spin one, also becomes SU(2) symmetric.[45] Even in the Q1D case, the model has an additional SU(2) symmetry, which is shown explicitly in Sec. II B 3. The G_{cs} coupling represents the spin-charge coupling term in the 1D case as seen from the bosonization technique.[46] In the notation of Eq. (2.10), the conditions of the hermitian (2.9) can be expressed as $g_{\nu(q,k_1,k_2)} = g_{\nu(q,k_2,k_1)}$, for $\nu = \rho, \sigma, s$ and $g_{\nu(q,k_1,k_2)} = g_{\nu(-q,\pi-k_2,\pi-k_1)}$ for $\nu = c, cs$. The number of independent coupling constants g_i in Eq. (2.8) is $5N_\perp^2(N_\perp+1)/2$.

B. Symmetry arguments

The Hubbard model (2.1) is known to have high symmetries, however, the g-ology Hamiltonian (2.8) is generalized one including low symmetry. Reflecting symmetries that the Hubbard model has, there appear several constraints on the g-ological couplings and the resultant RG equations can be simplified. In this subsection, we clarify relations for the coupling constants protected by the symmetries.

1. Spin-rotational SU(2)

The Hubbard model (2.1) is invariant under spin-rotation, while the g-ology Hamiltonian (2.8) includes the spin-anisotropic case. The spin-rotational symmetry can be argued

in terms of the generators of the spin rotation which are nothing but the spin operator:

$$\boldsymbol{S} = \frac{1}{2}\sum_{\boldsymbol{k},s_1,s_2} c^\dagger_{s_1}(\boldsymbol{k})\,\boldsymbol{\sigma}_{s_1,s_2} c_{s_2}(\boldsymbol{k}). \tag{2.13}$$

The arbitrary global spin rotation by these generators can be represented by the SU(2) matrix:

$$\begin{pmatrix} c_{j,l,\uparrow} \\ c_{j,l,\downarrow} \end{pmatrix} \to \begin{pmatrix} a_\sigma & b_\sigma \\ -b^*_\sigma & a^*_\sigma \end{pmatrix} \begin{pmatrix} c_{j,l,\uparrow} \\ c_{j,l,\downarrow} \end{pmatrix}, \tag{2.14}$$

where a_σ and b_σ are complex numbers satisfying $|a_\sigma|^2 + |b_\sigma|^2 = 1$. Obviously the Hubbard Hamiltonian (2.1) is invariant under the transformation (2.14). By requiring the g-ology Hamiltonian (2.8) to be invariant under this rotation, we obtain the constraints on the coupling constants. In the notation (2.10), the constraint relations are given by

$$g_{s(q,k_1,k_2)} = g_{\sigma(q,k_1,k_2)}, \tag{2.15a}$$

$$g_{c(q,k_1,k_2)} - g_{c(\pi-q+k_1+k_2,k_1,k_2)} = g_{cs(q,k_1,k_2)} - g_{cs(\pi-q+k_1+k_2,k_1,k_2)}. \tag{2.15b}$$

Since the property of the spin-rotational invariance is hold under the RG procedure, these relations can be considered as constraints on the renormalized coupling constants.

2. *Particle-hole symmetry*

The present bipartite half-filled system is invariant under the particle-hole transformation $c_s(\boldsymbol{k}) \leftrightarrow c^\dagger_s\big((\pi,\pi) - \boldsymbol{k}\big)$, where $c_s(\boldsymbol{k})$ is the Fourier transform of $c_{j,l,s}$. In the linearized dispersion (2.6), this particle-hole transformation corresponds to

$$c_{p,s}(\boldsymbol{k}) \leftrightarrow c^\dagger_{p,s}\big((p\pi,\pi) - \boldsymbol{k}\big). \tag{2.16}$$

In order to make this particle-hole symmetry meaningful, the number of chains $N_\perp$ must be even, otherwise the $k_\perp$ [Eq. (2.4)] cannot become symmetric in this transformation. By imposing the condition that the g-ology Hamiltonian (2.8) is invariant under this rotation, we obtain the constraints, in the notation (2.10),

$$g_{\nu(q,k_1,k_2)} \;=\; g_{\nu(-q,\pi-k_1,\pi-k_2)}, \tag{2.17}$$

where $\nu = \rho, \sigma, c, s, cs$. We note that, by combining the relation $g_{c/cs(q,k_1,k_2)} = g_{c/cs(-q,\pi-k_2,\pi-k_1)}$ [obtained from Eq. (2.9)], we find $g_{c/cs(q,k_1,k_2)} = g_{c/cs(q,k_2,k_1)}$.

3. *Pseudospin SU(2)*

In addition to the particle-hole symmetry, the system has an additional symmetry, if the interaction is on-site one only.[47] The generators of this SU(2) are given by[47]

$$Q^x \equiv \frac{\eta^\dagger + \eta}{2}, \quad Q^y \equiv \frac{\eta^\dagger - \eta}{2i}, \tag{2.18a}$$

$$Q^z \equiv \frac{1}{2}\sum_{\boldsymbol{k},s} :c^\dagger_s(\boldsymbol{k})\, c_s(\boldsymbol{k}):, \tag{2.18b}$$

where the so-called η-pairing operator is given by

$$\eta \equiv \sum_{\boldsymbol{k}} c_\uparrow(\boldsymbol{k})\, c_\downarrow\big((\pi,\pi) - \boldsymbol{k}\big). \tag{2.19}$$

The arbitrary rotation by these generators can be represented by the SU(2) matrix:

$$\begin{pmatrix} c_{j,l,\uparrow} \\ c^\dagger_{j,l,\downarrow} \end{pmatrix} \to \begin{pmatrix} a_\rho & z_{j,l} b_\rho \\ -z_{j,l} b^*_\rho & a^*_\rho \end{pmatrix} \begin{pmatrix} c_{j,l,\uparrow} \\ c^\dagger_{j,l,\downarrow} \end{pmatrix}, \tag{2.20}$$

where a_ρ and b_ρ are complex numbers satisfying $|a_\rho|^2 + |b_\rho|^2 = 1$, and $z_{j,l} = (-1)^{j+l}$. This transformation commutes with Eq. (2.14). One easily finds that this symmetry breaks down if the Hubbard model is extended, e.g., by including an additional intersite interaction. In the Fourier space with the linearized dispersion, the transformation (2.20) corresponds to

$$c_{p,\uparrow}(\boldsymbol{k}) \;\to\; a_\rho c_{p,\uparrow}(\boldsymbol{k}) + b_\rho c^\dagger_{p,\downarrow}\big((p\pi,\pi) - \boldsymbol{k}\big), \tag{2.21a}$$

$$c^\dagger_{p,\downarrow}(\boldsymbol{k}) \;\to\; a^*_\rho c^\dagger_{p,\downarrow}(\boldsymbol{k}) - b^*_\rho c_{p,\uparrow}\big((p\pi,\pi) - \boldsymbol{k}\big). \tag{2.21b}$$

The kinetic term (2.5) is invariant under this transformation. By imposing the condition that the g-ology Hamiltonian (2.8) is invariant under this transformation, we obtain

$$g_{c(q,k_1,k_2)} + g_{c(\pi-q+k_1+k_2,k_1,k_2)} = +g_{\rho(q,k_1,k_2)} + g_{\rho(\pi-q+k_1+k_2,k_1,k_2)}, \tag{2.22a}$$

$$g_{c(q,k_1,k_2)} - g_{c(\pi-q+k_1+k_2,k_1,k_2)} = -g_{\sigma(q,k_1,k_2)} + g_{\sigma(\pi-q+k_1+k_2,k_1,k_2)}, \tag{2.22b}$$

$$g_{s(q,k_1,k_2)} - g_{s(\pi-q+k_1+k_2,k_1,k_2)} = -g_{cs(q,k_1,k_2)} + g_{cs(\pi-q+k_1+k_2,k_1,k_2)}. \tag{2.22c}$$

The first relation is a natural extension to the known relation for the purely 1D case.[45] The last two relations, which do not appear in the 1D limit, imply that the couplings g_c and g_σ (g_s and g_{cs}) are not independent and related to each other.

The relations (2.22) can also be derived from the spin SU(2) relations (2.15) by using the charge-spin duality relation, as explicitly shown in the Appendix A.

C. Two-loop RG theory for the 1D Hubbard model

We briefly recall the known results of the two-loop RG theory for the purely 1D case, by focusing on the half-filled 1D Hubbard model:

$$H_{\rm 1D} = -t\sum_{j,s}\Big(c^\dagger_{j,s}c_{j+1,s} + \text{H.c.}\Big) + U\sum_{j,l} n_{j,\uparrow}n_{j,\downarrow}, \tag{2.23}$$

where $c_{j,s}$ is the annihilation operator of electron on the jth site with spin s, and $n_{j,s} = c^\dagger_{j,s}c_{j,s} - \frac{1}{2}$. The linearized dispersion is $\varepsilon(k) = -2t\cos k \to v(\pm k_\parallel - k_F)$ where the Fermi velocity and the Fermi momentum are $v = 2t$ and $k_F = \pi/2$. The g-ological scattering matrices are the same as Fig. 2 and we introduce $g_\rho \equiv (g_{2\perp} + g_\parallel)$, $g_\sigma \equiv (g_{2\perp} - g_\parallel)$, $g_c \equiv g_{3\perp}$,

$g_s \equiv g_{1\perp}$, and $g_{cs} \equiv g_{3\parallel}$, as before. The two-loop RG equations for the respective couplings are given by[3]

$$\frac{d}{dl}G_\rho = +2G_c^2 - 2G_\rho G_c^2, \tag{2.24a}$$
$$\frac{d}{dl}G_c = +2G_\rho G_c - G_\rho^2 G_c - G_c^3, \tag{2.24b}$$
$$\frac{d}{dl}G_\sigma = -2G_s^2 - 2G_\sigma G_s^2, \tag{2.24c}$$
$$\frac{d}{dl}G_s = -2G_\sigma G_s - G_\sigma^2 G_s - G_s^3, \tag{2.24d}$$

where l is the scaling parameter and the initial values are given by $G_i(0) = g_i/(2\pi v)$. We have neglected the G_{cs} coupling, since this has an irrelevant canonical dimension.[46]

These RG equations can be simplified reflecting the symmetries of the system. The spin-rotational SU(2) symmetry ensures $G_\sigma(l) = G_s(l)$, which is obtained from Eq. (2.15a) by neglecting the transverse momentum dependences. This relation holds even under the scaling procedure. The particle-hole symmetric Hubbard model has another pseudospin SU(2) symmetry and then the total Hamiltonian is characterized by the SU(2)×SU(2) symmetry.[45] This pseudospin SU(2) symmetry ensures $G_\rho(l) = G_c(l)$, which can be obtained from Eq. (2.22a), and thus this can be considered as the "charge" SU(2) symmetry. In this SU(2)× SU(2) symmetric case, the RG equations (2.24) can be simplified as

$$\frac{d}{dl}G_\rho = +2G_\rho^2 - 2G_\rho^3, \tag{2.25a}$$
$$\frac{d}{dl}G_\sigma = -2G_\sigma^2 - 2G_\sigma^3, \tag{2.25b}$$

where the initial values are given by $G_\rho(0) = G_\sigma(0) = U/(2\pi v)$. For repulsive interaction $U > 0$, one finds from Eq. (2.25) that the $G_\sigma(l)$ coupling decreases under scaling and is marginally irrelevant, while $G_\rho(l)$ is marginally relevant. The relevance/irrelevance of the couplings reflects the low-energy properties having finite/zero excitation gap in the corresponding modes. This behavior correctly reflects the properties of the 1D Mott insulator, where only the charge degrees of freedom is frozen due to the finite Mott gap and the spin has gapless excitations. By integrating out Eq. (2.25a) analytically from $l = 0$ to $l = l_\rho \equiv \ln(\Lambda/\Delta_\rho)$, one can obtain the characteristic energy scale Δ_ρ as

$$\Delta_\rho = C_\rho \Lambda \sqrt{G_\rho} \exp(-1/2G_\rho), \tag{2.26}$$

where C_ρ is an integration constant depending on $G_\rho(l_\rho)$. This formula reproduces the exactly known Mott gap in one dimension in the weak U region, since the U dependence of Δ_ρ is given by $\Delta_\rho \propto \sqrt{t_\parallel U}\exp(-2\pi t_\parallel/U)$.[48]

III. FORMULATION OF RENORMALIZATION GROUP

In this section, we derive the RG equations for the Q1D half-filled Hubbard model in the two-loop level based on the Kadanoff-Wilson cutoff scaling scheme.[1] In the one-loop level, the formulation for the Q1D case is found in Refs. 21,22,23,24,25,26. In this scheme, we take partial integration of the partition function over the fermion degrees of freedom in the outer energy shell and scale the bandwidth cutoff Λ as $\Lambda_l = \Lambda e^{-l}$ where l is the scaling parameter. We perform the logarithmic approximation, i.e., we keep the diagrams which become logarithmic singular in the 1D limit and thus the resultant Q1D RG equations are natural extensions to those for purely 1D case. In order to simplify the notations, we introduce the dimensionless couplings $G_{\nu(q,k_1,k_2)} \equiv g_{\nu(q,k_1,k_2)}/2\pi v$, where $\nu = \rho, \sigma, c, s, cs$.

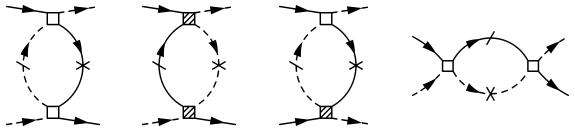

FIG. 3: The second-order diagrams contributing to the vertex corrections. The open square is the vertex for forward and backward scatterings, i.e., $g_{1\perp}$, $g_{2\perp}$, and $g_\parallel$, and the shaded square is the one for umklapp scattering $g_{3\perp}$ and $g_{3\parallel}$. The solid (dashed) line refers to a right-moving (left-moving) electron, $p = +(-)$. The slashed line represents that the electron has energies in the shell $\Lambda_{l+dl} < |\varepsilon_p(\boldsymbol{k})| < \Lambda_l$, while the crossed line represents the electron having high energies determined by the momentum conservation. The diagrams where the crossed line and slashed line are interchanged are also taken into account.

A. Peierls and Cooper bubbles in the one-loop level

First we focus on the one-loop contributions due to the second-order vertex corrections. Possible Peierls and Cooper bubble contributions, due to the normal and umklapp scattering, are shown in Fig. 3. We integrate out the electron degrees of freedom which have energy in the shell $\Lambda_{l+dl} < |\varepsilon_p(\boldsymbol{k})| < \Lambda_l$. The respective Peierls and Cooper bubbles have the *transverse*-momentum (i.e., patch-index) dependence of the external variables, as discussed in the literature.[21,22,23,24] This effect is crucial to induce the transverse-momentum dependence of the coupling constants. There remain ambiguities in the selection of the *longitudinal* momenta for the external variable, since, in general, all the momenta of vertex cannot be set on the Fermi surface if the Fermi surface is warped.[26] In this paper, we set three of four external momenta being on the Fermi surface and the longitudinal momentum conservation for each vertex (even for the internal momenta) is also considered. The choice of the external longitudinal momenta, in addition to the transverse momenta, affects on the internal momenta and also on the RG equations. To keep the symmetries discussed in the preceding section, we also take into account the different choice of three of four longitudinal momenta on the Fermi surface. The explicit form of the Peierls bubble is given by $-(T/V)\sum_{\boldsymbol{k}}^{\text{o.s.}}\sum_n \mathcal{G}_{0+}(\boldsymbol{k}, i\omega_n)\mathcal{G}_{0-}(\boldsymbol{k}-\boldsymbol{q}, i\omega_n)$ where $\mathcal{G}_{0p}(\boldsymbol{k}, i\omega_n) = [i\omega_n - \varepsilon_p(\boldsymbol{k})]^{-1}$ is the Green's function for the noninteracting case. By taking summation of the Matsubara frequency and by performing the outer-shell integral over constant energy, this Peierls bubble contribution is given

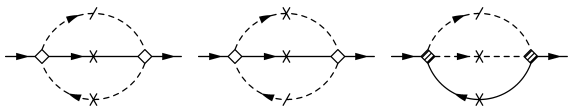

FIG. 4: The logarithmic-singular second-order diagrams for the Green's function, contributing the self energy. The notations are the same as in Fig. 3. Other types of second-order diagrams are not logarithmic singular even in the 1D limit and can be neglected.

by $(2\pi v N_\perp)^{-1}\sum_k I_{(q,k,k_1,k_2)}dl$, where the cutoff function $I_{(q,k,k_1,k_2)}$ is given in the $T\to 0$ limit by

$$I_{(q,k,k_1,k_2)} = \frac{\Lambda}{2}\sum_{p=\pm}\sum_{i=1,2}\frac{\Theta\big(\Lambda + pA_{q,k,k_i}(l)\big)}{2\Lambda + pA_{q,k,k_i}(l)}. \quad (3.1)$$

The quantity $A_{q,k,k'}(l)$ being the functions of $t_\perp(l)$ is given by

$$\begin{aligned} A_{q,k,k'}(l) \;\equiv\; & 2t_\perp(l)[\cos k + \cos(k-q)] \\ & - 2t_\perp(l)[\cos k' + \cos(k'-q)]. \end{aligned} \quad (3.2)$$

The second term in the rhs of $A_{q,k,k'}(l)$ appears due to the longitudinal momentum conservation. In the conventional approach, this term has been neglected,[21,22,23,24] however is crucial to reproduce the known RG equations in the two-leg ladder system (Sec. IV). We note $I_{(q,k,k_1,k_2)}=1$ in the 1D limit ($t_\perp\to 0$). The Cooper bubble contribution is also calculated in a similar way and can be expressed, after some algebra, as $-I_{(\pi-q+k_1+k_2,k',k_1,k_2)}$ where we have used the particle-hole symmetry.

B. Two-loop self-energy corrections

To go beyond the one-loop RG theory, we have to take into account two-loop self-energy corrections based on the second-order perturbation. The Fermi surface deformation can be taken into account by considering these corrections and has been discussed intensively by Dusuel and Douçot,[26] based on the zero-temperature formalism. Here we perform the finite-temperature formalism and take the $T\to 0$ limit at the final stage of the calculation. The second-order self-energy diagrams are shown in Fig. 4. In the second-order perturbation, there are two types of corrections to the single-particle Green's function $\mathcal{G}$: One is the corrections to the wave-function renormalization factor while the other contributes to the renormalization of the velocity and the interchain hopping. In the present RG scheme, the renormalization factor can have a transverse momentum dependence. So we assume that the Green's function takes a form

$$\mathcal{G}_p(\boldsymbol{k}, i\omega_n) = \frac{z^p_{k_\perp}}{i\omega_n - v(pk_\parallel - k_F) + 2t_\perp^{\rm eff}\cos k_\perp}. \quad (3.3)$$

where $z^R_{k_\perp} = z^L_{-k_\perp}(\equiv z_{k_\perp})$. The explicit calculation of outer shell integration of the diagrams in Fig. 4 yields

$$\mathcal{G}_R^{-1}(\boldsymbol{k}, i\omega_n) \;=\; \mathcal{G}_{0R}^{-1}(\boldsymbol{k}, i\omega_n) - \frac{dl}{2N_\perp^2}\sum_{q,k'} G^2_{\Sigma(q,k,k')}\left[J_{0(q,k,k')} - J_{1(q,k,k')}\mathcal{G}_{0R}^{-1}(\boldsymbol{k}, i\omega_n)\right], \quad (3.4)$$

for the right-moving electrons. The second-order coupling constants contributing the self-energy corrections are put into a form:

$$\begin{aligned} G^2_{\Sigma(q,k,k')} \;\equiv\; & G^2_{1\perp(q,k,k')} + G^2_{2\perp(q,k,k')} + G^2_{\parallel(q,k,k')} + \frac{1}{2}G^2_{3\perp(q,k,\pi-k')} + \frac{1}{2}G^2_{3\perp(\pi-q+k+k',k,\pi-k')} \\ & + \frac{1}{2}G^2_{3\parallel(q,k,\pi-k')} - G_{3\parallel(q,k,\pi-k')}G_{3\parallel(\pi-q+k+k',k,\pi-k')} + \frac{1}{2}G^2_{3\parallel(\pi-q+k+k',k,\pi-k')}. \end{aligned} \quad (3.5)$$

We note that the umklapp scattering with the same spins $G_{3\parallel}$ also has finite contributions which are absent in the 1D limit. The quantities $J_{0(q,k,k')}$ and $J_{1(q,k,k')}$ denote the cutoff functions due to the warped Fermi surface, which are also determined by the quantity $A_{q,k,k'}(l)$ [Eq. (3.2)]. These cutoff functions J_0 and J_1 take different forms depending on the relation between $A_{q,k,k'}(l)$ and Λ: For $|A_{q,k,k'}(l)|<\Lambda$, these are given by

$$J_{0(q,k,k')} \;=\; 2\Lambda\ln\left[\frac{4\Lambda + A_{q,k,k'}(l)}{4\Lambda - A_{q,k,k'}(l)}\right], \quad (3.6a)$$

$$J_{1(q,k,k')} \;=\; \frac{16\Lambda^2}{16\Lambda^2 - A^2_{q,k,k'}(l)}. \quad (3.6b)$$

For $|A_{q,k,k'}(l)|>\Lambda$,

$$J_{0(q,k,k')} \;=\; 2\Lambda\ln\left[\frac{4\Lambda + |A_{q,k,k'}(l)|}{2\Lambda + |A_{q,k,k'}(l)|}\right]\mathrm{sgn}\big(A_{q,k,k'}(l)\big), \quad (3.7a)$$

$$J_{1(q,k,k')} \;=\; \frac{2\Lambda}{4\Lambda + |A_{q,k,k'}(l)|} + \frac{2\Lambda}{2\Lambda + |A_{q,k,k'}(l)|}. \quad (3.7b)$$

There remain subtleties in the integral region of outer shell,[1] here we adopt the simplest shell integral following Ref. 4. The scaling deviation terms[1,4] have been neglected.

The self-energy corrections proportional to $\mathcal{G}_{0R}^{-1}(\boldsymbol{k}, i\omega_n)$ in Eq. (3.4) contribute to the wave-function renormalization fac-

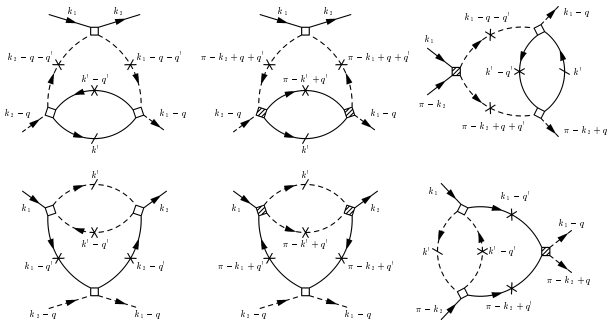

FIG. 5: The third-order diagrams contributing to the vertex corrections, which have an order $O(G^3 dl)$ in the 1D limit. The notations are the same as in Fig. 3. Other types of third-order diagrams have an order $O(G^3 dl^2)$ and can be neglected.

tor $z^p_{k_\perp}$. The explicit RG equation of the wave-function renormalization factor is given by

$$\frac{d}{dl}\ln z_k \;=\; -\frac{1}{2N_\perp^2}\sum_{q,k'} G^2_{\Sigma(q,k,k')}\, J_{1(q,k,k')}. \qquad (3.8)$$

The self-energy corrections proportional to J_0 in Eq. (3.4) contribute to the renormalization of the velocity and the Fermi surface deformation. To simplify discussions in the present analysis, we neglect the velocity renormalization, since this effect would only yield quantitative changes. The Fermi surface deformation can be extracted from these second-order corrections. Since the Fermi surface is given by Eq. (2.7), the Fermi surface deformation thus corresponds to the renormalization of the interchain hopping. By noting that the self-energy contributions to the interchain hopping should have transverse momentum dependence $\cos k$, the RG equation of the renormalization for the interchain hopping is given by

$$\frac{d}{dl}t_\perp(l) \;=\; t_\perp(l) - \frac{1}{4N_\perp^3}\sum_{q,k,k'} G^2_{\Sigma(q,k,k')}\, J_{0(q,k,k')}\cos k. \qquad (3.9)$$

The renormalization to higher-order interchain hopping has been neglected.

C. Two-loop RG equations

In order to complete the two-loop RG theory, one has to take into account the next-to-leading logarithmic contributions to the vertex part. The two-loop vertex corrections can be calculated in a similar way to that for the self-energy correction. The third-order diagrams with the next-to-leading logarithmic contributions are shown in Fig. 5 and yield the renormalization of the vertex as $G_{i(q,k_1,k_2)} \to z_{i(q,k_1,k_2)}\, G_{i(q,k_1,k_2)}$, where $i = 1\perp$, $2\perp$, $\|$, $3\perp$, and $3\|$. Other types of diagrams are of the order $O(G^3 dl^2)$ which are already taken into account in the one-loop level. As is well-known in the 1D case, the RG is formulated by deriving the scaling equations for the "renormalized" coupling constants $G_i(l) \equiv G_i z_i(l) z^2(l)$[1,3,4] where $z(l)$ is the wave-function renormalization factor. In the present Q1D RG, by keeping in mind that the vertex has a transverse-momentum dependence, the renormalized coupling constants are defined as

$$G_{i(q,k_1,k_2)}(l) \;\equiv\; G_{i(q,k_1,k_2)}\, z_{i(q,k_1,k_2)}(l) \times \sqrt{z^R_{k_1}(l)\, z^R_{k_2}(l)\, z^L_{k_1-q}(l)\, z^L_{k_2-q}(l)}\,, \qquad (3.10)$$

for the normal scatterings ($i = 1\perp, 2\perp, \|$), and

$$G_{i(q,k_1,k_2)}(l) \;\equiv\; G_{i(q,k_1,k_2)}\, z_{i(q,k_1,k_2)}(l) \times \sqrt{z^R_{k_1}(l)\, z^R_{k_2}(l)\, z^L_{k_1-q}(l)\, z^L_{k_2+q}(l)}\,, \qquad (3.11)$$

for the umklapp scatterings ($i = 3\perp, 3\|$). The wave-function renormalization factor $z^p_{k_\perp}$ comes from the rescaling of the electron field operator. Even in the two-loop vertex corrections, the cutoff function due to the warping of the Fermi surface appears, which is given by

$$J_{2(q+k'';k_1,k_2;k',k'')} \;=\; \frac{1}{2}J_{1(q+k''-k_1,k',k'')} + \frac{1}{2}J_{1(q+k''-k_2,k',k'')}. \qquad (3.12)$$

The cutoff function I, J_0, J_1, and J_2 are not universal and would take different forms depending on the RG formulation. The function I [Eq. (3.1)] is not continuous as a function of $A_{q,k,k_i}(l)$ which would be due to the sharp cutoff of the bandwidth. This unphysical discontinuity of I affects the results of the numerical integration of the RG equations. In order to avoid this unphysical effect, we replace I by a smooth function which reproduce the limiting behavior of Eq. (3.1) for small and large $A_{q,k,k_i}(l)$.

From the straightforward calculation of the diagrams in Fig. 5, we obtain the two-loop RG equations for $G_{1\perp(q,k_1,k_2)}$, $G_{2\perp(q,k_1,k_2)}$, $G_{\|(q,k_1,k_2)}$, $G_{3\perp(q,k_1,k_2)}$, and $G_{3\|(q,k_1,k_2)}$. We note that, if we set $N_\perp = 2$ and if we neglect the umklapp scattering $G_{3\perp(q,k_1,k_2)}$ and $G_{3\|(q,k_1,k_2)}$, our RG equations reproduce the two-loop RG equations obtained by Fabrizio[33] in the two-leg ladder system at away from half filling. By using Eq. (2.10), we rewrite the RG equation in terms of G_ρ, G_σ, G_c, G_s, and G_{cs}. For the system with the spin-rotational SU(2) symmetry, the coupling constants satisfy the relations given by Eq. (2.15). The full RG equations in this case is given in the Appendix B. For the particle-hole symmetric Hubbard model, the coupling constants also satisfy the relations (2.17) and (2.22). By using all these relations, the RG equations with the SU(2) × SU(2) symmetry are extremely simplified. The complete two-loop RG equations for the coupling constants $G_{\rho(q,k_1,k_2)}$ and $G_{\sigma(q,k_1,k_2)}$ are given by

$$
\begin{aligned}
\frac{d}{dl}G_{\nu(q,k_1,k_2)} &= \frac{1}{2N_\perp}\sum_{k'}\left[\alpha_{\nu(q;k_1,k_2;k')}I_{(q,k',k_1,k_2)} - \beta_{\nu(q;k_1,k_2;k')}I_{(\pi-q+k_1+k_2,k',k_1,k_2)}\right] \\
&\quad - \frac{1}{4N_\perp^2}G_{\nu(q,k_1,k_2)}\sum_{q',k'}\left[G^2_{\Sigma(q',k_1,k')}J_{1(q',k_1,k')} + G^2_{\Sigma(q',k_2,k')}J_{1(q',k_2,k')}\right] \\
&\quad - \frac{1}{4N_\perp^2}G_{\nu(q,k_1,k_2)}\sum_{q',k'}\left[G^2_{\Sigma(q',-k_1+q,k')}J_{1(q',-k_1+q,k')} + G^2_{\Sigma(q',-k_2+q,k')}J_{1(q',-k_2+q,k')}\right] \\
&\quad + \frac{1}{4N_\perp^2}\sum_{q',k'}\Big\{\left[G_{\nu(q+q',k_1,k_2)} - \Theta_\nu G_{\nu(\pi-q-q'+k_1+k_2,k_1,k_2)}\right]\gamma_{\nu(q-k_1+k',q-k_2+k';k',k';q')} \\
&\qquad\quad - \frac{1}{2}G_{\nu(\pi-q-q'+k_1+k_2,k_1,k_2)}\delta_{\nu(q-k_1+k',q-k_2+k';k',k';q')}\Big\}J_{2(q+k';k_1,k_2;k',k'-q')} \\
&\quad + \frac{1}{4N_\perp^2}\sum_{q',k'}\Big\{\left[G_{\nu(q-q',k_1-q',k_2-q')} - \Theta_\nu G_{\nu(\pi-q-q'+k_1+k_2,k_1-q',k_2-q')}\right]\gamma_{\nu(k_1-k',k_2-k';k_1,k_2;q')} \\
&\qquad\quad - \frac{1}{2}G_{\nu(\pi-q-q'+k_1+k_2,k_1-q',k_2-q')}\delta_{\nu(k_1-k',k_2-k';k_1,k_2;q')}\Big\}J_{2(k';k_1,k_2;k',k'-q')}, \qquad (3.13)
\end{aligned}
$$

where $\nu = \rho, \sigma$ and the sign function Θ_ν is $\Theta_\rho = +1$ and $\Theta_\sigma = -1$. The index of the scaling parameter l in the coupling constants $G_{\nu(q,k_1,k_2)}$ is suppressed. The coupling constants for the self-energy corrections, Eq. (3.5), can be rewritten in terms of G_ρ and G_σ, as

$$
G^2_{\Sigma(q,k,k')} = G^2_{\rho(q,k,k')} + \frac{1}{2}G_{\rho(q,k,k')}G_{\rho(\pi-q+k+k',k,k')} + 3G^2_{\sigma(q,k,k')} - \frac{3}{2}G_{\sigma(q,k,k')}G_{\sigma(\pi-q+k+k',k,k')}. \qquad (3.14)
$$

The quantities α_ν, β_ν, γ_ν, and δ_μ ($\nu = \rho, \sigma$) are defined as follows. The quantities α_ν represent the one-loop Peierls bubble contributions given by

$$
\begin{aligned}
\alpha_{\rho(q;k_1,k_2;k')} &\equiv 2G_{\rho(q,k_1,k')}G_{\rho(q,k',k_2)} + G_{\rho(q,k_1,k')}G_{\rho(\pi-q+k_2+k',k',k_2)} + G_{\rho(\pi-q+k_1+k',k_1,k')}G_{\rho(q,k',k_2)} \\
&\quad + 6G_{\sigma(q,k_1,k')}G_{\sigma(q,k',k_2)} - 3G_{\sigma(q,k_1,k')}G_{\sigma(\pi-q+k_2+k',k',k_2)} - 3G_{\sigma(\pi-q+k_1+k',k_1,k')}G_{\sigma(q,k',k_2)} \\
&\quad + G_{\rho(\pi-q+k_1+k',k_1,k')}G_{\rho(\pi-q+k_2+k',k',k_2)} + 3G_{\sigma(\pi-q+k_1+k',k_1,k')}G_{\sigma(\pi-q+k_2+k',k',k_2)}, \\
\alpha_{\sigma(q;k_1,k_2;k')} &\equiv 2G_{\rho(q,k_1,k')}G_{\sigma(q,k',k_2)} + 2G_{\sigma(q,k_1,k')}G_{\rho(q,k',k_2)} - 4G_{\sigma(q,k_1,k')}G_{\sigma(q,k',k_2)} \\
&\quad - G_{\rho(q,k_1,k')}G_{\sigma(\pi-q+k_2+k',k',k_2)} - G_{\sigma(\pi-q+k_1+k',k_1,k')}G_{\rho(q,k',k_2)} + 2G_{\sigma(q,k_1,k')}G_{\sigma(\pi-q+k_2+k',k',k_2)} \\
&\quad + G_{\rho(\pi-q+k_1+k',k_1,k')}G_{\sigma(q,k',k_2)} + G_{\sigma(q,k_1,k')}G_{\rho(\pi-q+k_2+k',k',k_2)} + 2G_{\sigma(\pi-q+k_1+k',k_1,k')}G_{\sigma(q,k',k_2)} \\
&\quad - G_{\rho(\pi-q+k_1+k',k_1,k')}G_{\sigma(\pi-q+k_2+k',k',k_2)} - G_{\sigma(\pi-q+k_1+k',k_1,k')}G_{\rho(\pi-q+k_2+k',k',k_2)} \\
&\quad - 2G_{\sigma(\pi-q+k_1+k',k_1,k')}G_{\sigma(\pi-q+k_2+k',k',k_2)}.
\end{aligned}
$$

The quantities β_ν represent the one-loop Cooper bubble contributions:

$$
\begin{aligned}
\beta_{\rho(q;k_1,k_2;k')} &\equiv G_{\rho(q-k_2+k',k_1,k')}G_{\rho(q-k_1+k',k',k_2)} + 3G_{\sigma(q-k_2+k',k_1,k')}G_{\sigma(q-k_1+k',k',k_2)}, \\
\beta_{\sigma(q;k_1,k_2;k')} &\equiv G_{\rho(q-k_2+k',k_1,k')}G_{\sigma(q-k_1+k',k',k_2)} + G_{\sigma(q-k_2+k',k_1,k')}G_{\rho(q-k_1+k',k',k_2)} \\
&\quad + 2G_{\sigma(q-k_2+k',k_1,k')}G_{\sigma(q-k_1+k',k',k_2)}.
\end{aligned}
$$

Finally the quantities γ_ν and δ_ν represent the two-loop vertex contributions:

$$
\begin{aligned}
\gamma_{\rho(q_1,q_2;k_1,k_2;q')} &\equiv G_{\rho(q_1,k_1,k_1-q')}G_{\rho(q_2,k_2,k_2-q')} + 3G_{\sigma(q_1,k_1,k_1-q')}G_{\sigma(q_2,k_2,k_2-q')}, \\
\gamma_{\sigma(q_1,q_2;k_1,k_2;q')} &\equiv G_{\rho(q_1,k_1,k_1-q')}G_{\rho(q_2,k_2,k_2-q')} - G_{\sigma(q_1,k_1,k_1-q')}G_{\sigma(q_2,k_2,k_2-q')}, \\
\delta_{\rho(q_1,q_2;k_1,k_2;q')} &\equiv G_{\rho(q_1,k_1,k_1-q')}G_{\rho(\pi-q_2-q'+2k_2,k_2,k_2-q')} + G_{\rho(\pi-q_1-q'+2k_1,k_1,k_1-q')}G_{\rho(q_2,k_2,k_2-q')} \\
&\quad - 3G_{\sigma(q_1,k_1,k_1-q')}G_{\sigma(\pi-q_2-q'+2k_2,k_2,k_2-q')} - 3G_{\sigma(\pi-q_1-q'+2k_1,k_1,k_1-q')}G_{\sigma(q_2,k_2,k_2-q')}, \\
\delta_{\sigma(q_1,q_2;k_1,k_2;q')} &\equiv -G_{\rho(q_1,k_1,k_1-q')}G_{\rho(\pi-q_2-q'+2k_2,k_2,k_2-q')} - G_{\rho(\pi-q_1-q'+2k_1,k_1,k_1-q')}G_{\rho(q_2,k_2,k_2-q')} \\
&\quad - G_{\sigma(q_1,k_1,k_1-q')}G_{\sigma(\pi-q_2-q'+2k_2,k_2,k_2-q')} - G_{\sigma(\pi-q_1-q'+2k_1,k_1,k_1-q')}G_{\sigma(q_2,k_2,k_2-q')}.
\end{aligned}
$$

We have only kept the marginal scattering processes. In the purely 1D case, it is known that the G_{cs} term has ir-

relevant canonical dimension.[46] In the present case, some of the $G_{cs(q,k_1,k_2)}$ couplings have a marginal canonical dimension, however, the RG equation for the $G_{cs(q,k_1,k_2)}$ does not appear explicitly since the correction due to this term always appears in a form $(G_{cs(q,k_1,k_2)} - G_{cs(\pi-q+k_1+k_2,k_1,k_2)})$, which shows the same l-dependence of $(-G_{\sigma(q,k_1,k_2)} + G_{\sigma(\pi-q+k_1+k_2,k_1,k_2)})$, as seen from Eqs. (2.15a) and (2.22c). For $N_\perp = 8$, e.g., the number of independent coupling constants reduces to 300 instead of 1440 for without assuming the symmetries. If the transverse momentum dependences of the coupling constants are neglected, the 1D RG equations [Eq. (2.25)] are reproduced.

From the numerical integration of the RG equations, we can estimate characteristic energy scales. Here we focus on the renormalized interchain hopping and the charge/spin excitation gaps. The effective renormalized interchain hopping is given by

$$t_\perp^{\rm eff} \equiv \Lambda \exp(-l_\perp), \tag{3.15}$$

where the quantity $l_\perp$ is determined from $t_\perp(l_\perp) = \Lambda$. In the noninteracting limit, the interchain hopping scales as $t_\perp(l) = t_\perp e^l$, then $l_\perp = \ln(\Lambda/t_\perp)$ and the effective interchain hopping trivially reduces to the bare interchain hopping $t_\perp^{\rm eff} = t_\perp$. This quantity characterizes the dimensional-crossover energy scale, below which the system cannot be regarded as a one-dimensional system any more. In addition, the Fermi surface deformation can be determined by this quantity. By noting the relation (2.7), the deformed Fermi surface is given by

$$k_F^{\rm eff}(k_\perp) = k_F + 2\frac{t_\perp^{\rm eff}}{v}\cos k_\perp. \tag{3.16}$$

It is known that the Fermi-surface deformation comes only from the renormalization in the high-energy regime, since the coupling constants which appear in the rhs of Eq. (3.9) are the irrelevant couplings.[26]

In the present RG scheme, the information of the charge gap Δ_ρ and the spin gap Δ_σ can be extracted by focusing on the combination of the coupling constants:

$$G_{\nu+} \equiv \frac{1}{N_\perp^2}\sum_{k,k'} G_{\nu(k-k',k,k)}, \tag{3.17}$$

where $\nu = \rho, \sigma$. This interpretation can be justified by noting that the uniform charge/spin susceptibility is determined by these quantities[25] and by the field-theoretical approach for the two-leg ladder ($N_\perp = 2$) case as will be shown in Sec. IV. A typical scaling flow is shown in Fig. 6, where we have set $N_\perp = 8$. As a reference, the scaling flow for the 1D case is also shown. The charge coupling $G_{\rho+}$ shows similar behavior to that in the 1D case, while the spin coupling $G_{\sigma+}$ becomes relevant and have a finite fixed point value $G^*_{\sigma-} = -1$. We note that the magnitude of several coupling constants becomes large and exceed the unity under the scaling procedure for $l > l_\perp$. By focusing on this scaling behavior of $G_{\nu+}(l)$, we can estimate the magnitude of the excitation gaps by

$$\Delta_\nu \equiv \Lambda \exp(-l_\nu) \tag{3.18}$$

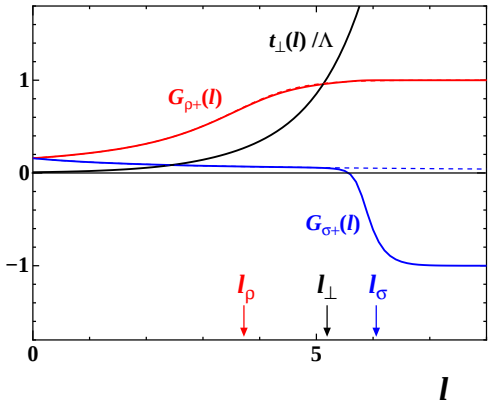

FIG. 6: (Color online) The scaling flows of the coupling constants $G_{\rho+}(l)$ and $G_{\sigma+}(l)$ and the interchain hopping $t_\perp(l)/\Lambda$ for $N_\perp = 8$ with fixed $U/t_\parallel = 2$ and $t_\perp/t_\parallel = 0.05$. The case for $t_\perp = 0$ is shown by the dotted lines.

where the quantity l_ν is determined from $|G_{\nu+}(l_\nu)| = c$ where c is a numerical constant. In the present numerical calculations, we will set $c = 0.7$ and $\Lambda = 2vk_F$. As seen in Eq. (2.26), these ambiguity simply affects on the numerical factor and our choice reproduce well the exact results of the Δ_ρ in the 1D case.[48] The interchain-hopping dependence of Δ_ρ, Δ_σ, and $t_\perp^{\rm eff}$ is shown in Fig. 7. The charge gap is suppressed due to the interchain hopping but is always finite even when the interchain hopping exceeds the magnitude of the charge gap. In the present bipartite Q1D half-filled Hubbard model, we find that the charge gap is always finite for $U > 0$. This is contrast to the results obtained from the chain-DMFT[27,28,29,30] where the metal-insulator (Mott) transition has been suggested for finite interchain hopping at $T = 0$. This difference would arise from the difference in the treatment of the Fermi-surface nesting of the system. In the present model, the Fermi surface is always nested perfectly even for the finite interchain hopping where the nesting vector is (π, π). In our approach, we fully take into account this effect, however in the chain-DMFT, the warping of the Fermi surface is not taken into account. We expect that the Fermi-surface nesting would play crucial roles in the Q1D Mott transition, since the 1D Mott insulator itself is realized even in the small U region due to the commensurability effect, which would be sensitive to the Fermi-surface nesting. By means of the present Q1D RG scheme, the effect of the nesting deviation will be reported elsewhere.[49]

IV. TWO-LEG LADDER MODEL

To indicate the validity of the two-loop RG equations obtained in the preceding section, we apply it to the two-leg Hubbard ladder model with a bipartite lattice. This model has been investigated by the RG method combined with the analytical field-theoretical method[34,35,36,37,38] and by the numerical DMRG method,[43,44] and it has been clarified that the spin-gapped insulating state called the D-Mott phase is realized. Lin, Balents and Fisher obtained the highly symmetric

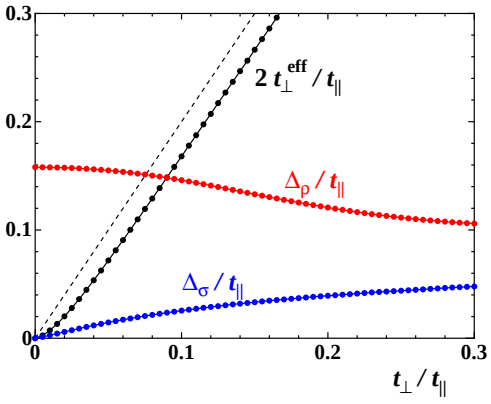

FIG. 7: (Color online) The charge gap Δ_ρ, the spin gap Δ_σ, and the characteristic energy scale $t_\perp^{\rm eff}$, as a function of $t_\perp/t_\parallel$ for $N_\perp = 8$ and $U/t_\parallel = 2$. The dashed line represents the magnitude of the bare interchain hopping.

SO(8) Gross-Neveu model as an effective theory in the low-energy limit by using the fixed-point behavior of the one-loop RG analysis.[38] They further discussed finite-energy spectrum based on this effective theory, however, it is not clear that this high symmetry still holds at finite-energy scale. Actually, the RG method allows us to study the characteristic energy scales in addition to the fixed point behavior, however, the naive one-loop RG is not sufficient to estimate the excitation gaps, since the RG method breaks down at the scale corresponding to the largest gap, as mentioned before. A promising method is to derive an effective theory by tracing out the gapped modes based on the field-theoretical treatment. However, in the present two-loop RG, the excitation gaps in the respective modes can be estimated without following the tracing-out procedure. This is not so trivial if the respective modes are not independent. In this section, in order to check the validity of the present method, we consider the two-leg ladder system, which is a minimal model of the spin-charge coupled systems, and confirm that this two-loop RG theory reproduces results obtained by the DMRG method and further analyze the excitation properties in detail by combining the field-theoretical bosonization and fermionization method.

The model can be obtained from Eq. (2.1) by simply setting $N_\perp = 2$. The possible values of the transverse momentum are $k_\perp = 0$ and π. From the symmetry requirements [Eqs. (2.15), (2.17), and (2.22)], the number of independent coupling constants reduces to 8 instead of 30 for without assuming the symmetries. To respect these symmetries and to make the physical picture transparent, we derive the effective low-energy theory by applying the bosonization and refermionization.[40,42,50]

First we apply the conventional Abelian bosonization to the Hamiltonian. The field operators of the right and left-moving electrons are written as

$$\psi_{p,s,\zeta}(x) = \frac{\eta_{s,\zeta}}{\sqrt{2\pi a}} \exp\left(ipk_{F,\zeta}x + ip\,\varphi_{p,s,\zeta}\right), \qquad (4.1)$$

where $p = +/-$ represents the right/left moving electron, s represents the spin, ζ represents the band index: $\zeta = +(-)$ for $k_\perp = 0(\pi)$, and $k_{F,\pm} = (\pi/2 \pm 2t_\perp/v)$ [see Eq. (2.7)]. The technical details can be found in Refs. 40 and 42. The chiral bosons obey the commutation relations $[\varphi_{p,s,\zeta}(x), \varphi_{p,s',\zeta'}(x')] = ip\pi\,\mathrm{sgn}(x-x')\,\delta_{s,s'}\,\delta_{\zeta,\zeta'}$ and $[\varphi_{+,s,\zeta}, \varphi_{-,s',\zeta'}] = i\pi\,\delta_{s,s'}\,\delta_{\zeta,\zeta'}$. The Klein factors $\eta_{s,\zeta}$, which satisfy $\{\eta_{s,\zeta}, \eta_{s',\zeta'}\} = 2\delta_{s,s'}\delta_{\zeta,\zeta'}$, are introduced in order to retain the correct anticommutation relation of the field operators between the different spin and band index. To express the electron fields in terms of the bosonic fields representing physical modes, we define a new set of chiral bosonic fields $\phi^p_{\rho+}$, $\phi^p_{\rho-}$, $\phi^p_{\sigma+}$, and $\phi^p_{\sigma-}$, by

$$\varphi_{p,s,\zeta} \equiv \phi^p_{\rho+} + \zeta\phi^p_{\rho-} + s\phi^p_{\sigma+} + s\zeta\phi^p_{\sigma-}, \qquad (4.2)$$

where $s = \uparrow/\downarrow = +/-$. The commutation relations for these bosonic fields are $[\phi^p_{\nu r}(x), \phi^p_{\nu' r'}(x')] = ip\,(\pi/4)\,\mathrm{sgn}(x-x')\,\delta_{\nu,\nu'}\delta_{r,r'}$ and $[\phi^+_{\nu r}(x), \phi^-_{\nu' r'}(x')] = i\,(\pi/4)\,\delta_{\nu,\nu'}\delta_{r,r'}$. From Eq. (4.1) the density operator is given by

$$:\psi^\dagger_{p,s,\zeta}\,\psi_{p,s,\zeta}: = \frac{1}{2\pi}\frac{d}{dx}\varphi_{p,s,\zeta}(x). \qquad (4.3)$$

The convention of the Klein factors is the same as Ref. 40. From this relation, one finds that the boson fields $\phi_{\rho\pm}$ can be interpreted to denote the "charge" degrees of freedom, while $\phi_{\sigma\pm}$ to denote the "spin" degrees of freedom.

To appreciate two SU(2) symmetries in the effective theory, we next fermionize the $\phi_{\sigma+}$, $\phi_{\sigma-}$, and $\phi_{\rho+}$ bosonic fields by introducing the Majorana fermions ξ^n_p ($n = 1, \cdots, 6$ and $p = R/L = +/-$):

$$\frac{1}{\sqrt{2}}\left(\xi^2_p + i\xi^1_p\right) \equiv \frac{\kappa_{\sigma+}}{\sqrt{2\pi a}}\exp\left(ip\,2\phi^p_{\sigma+}\right), \qquad (4.4a)$$

$$\frac{1}{\sqrt{2}}\left(\xi^4_p + i\xi^3_p\right) \equiv \frac{\kappa_{\sigma-}}{\sqrt{2\pi a}}\exp\left(ip\,2\phi^p_{\sigma-}\right), \qquad (4.4b)$$

$$\frac{1}{\sqrt{2}}\left(\xi^6_p + i\xi^5_p\right) \equiv \frac{\kappa_{\rho+}}{\sqrt{2\pi a}}\exp\left(ip\,2\phi^p_{\rho+}\right), \qquad (4.4c)$$

where $\kappa_{\nu\pm}$ is the Klein factor, satisfying $\{\kappa_{\nu r}, \kappa_{\nu' r'}\} = \delta_{\nu,\nu'}\delta_{r,r'}$ and $\kappa^2_{\nu r} = 1$. These Majorana fields satisfy the anticommutation relations: $\{\xi^n_p(x), \xi^{n'}_{p'}(x')\} = \delta(x-x')\,\delta_{p,p'}\,\delta_{n,n'}$. The Hamiltonian can be refermionized in terms of the Majorana fermions. Our new finding is that the two sets of three Majorana fields form triplets, due to the constraint of two SU(2) symmetries. So we define

$$\boldsymbol{\xi}_p \equiv (\xi^1_p, \xi^2_p, \xi^3_p), \quad \boldsymbol{\zeta}_p \equiv (\xi^4_p, \xi^5_p, \xi^6_p). \qquad (4.5)$$

The g-ology Hamiltonian $\int dx\,\mathcal{H}_{\rm ladder} = (H_0 + H_{\rm I})|_{N_\perp=2}$ [Eqs. (2.5) and (2.8) with $N_\perp = 2$] can be reexpressed in a highly symmetric form as

$$\begin{aligned}\mathcal{H}_{\rm ladder} &= -i\frac{v}{2}\left(\boldsymbol{\xi}_R\cdot\partial_x\boldsymbol{\xi}_R-\boldsymbol{\xi}_L\cdot\partial_x\boldsymbol{\xi}_L\right)-i\frac{v}{2}\left(\boldsymbol{\zeta}_R\cdot\partial_x\boldsymbol{\zeta}_R-\boldsymbol{\zeta}_L\cdot\partial_x\boldsymbol{\zeta}_L\right)+\frac{v}{\pi}\left[\left(\partial_x\phi^R_{\rho-}\right)^2+\left(\partial_x\phi^L_{\rho-}\right)^2\right]\\ &-\frac{g_{\sigma+}}{2}\left(\boldsymbol{\xi}_R\cdot\boldsymbol{\xi}_L\right)^2+\frac{g_{\rho+}}{2}\left(\boldsymbol{\zeta}_R\cdot\boldsymbol{\zeta}_L\right)^2+\frac{g_{\rho-}}{\pi^2}\left(\partial_x\phi^R_{\rho-}\right)\left(\partial_x\phi^L_{\rho-}\right)\\ &-g_{\sigma-}\left(\boldsymbol{\xi}_R\cdot\boldsymbol{\xi}_L\right)\left(\boldsymbol{\zeta}_R\cdot\boldsymbol{\zeta}_L\right)-\frac{ig_{\sigma(\pi,0,\pi)}}{2\pi a}\left(\boldsymbol{\xi}_R\cdot\boldsymbol{\xi}_L\right)\cos 2\theta_{\rho-}-\frac{ig_{\rho(\pi,0,\pi)}}{2\pi a}\left(\boldsymbol{\zeta}_R\cdot\boldsymbol{\zeta}_L\right)\cos 2\theta_{\rho-}\\ &+\frac{ig_{\sigma(0,0,\pi)}}{2\pi a}\left(\boldsymbol{\xi}_R\cdot\boldsymbol{\xi}_L\right)\cos(2\phi_{\rho-}+8t_\perp x/v)-\frac{ig_{\rho(0,0,\pi)}}{2\pi a}\left(\boldsymbol{\zeta}_R\cdot\boldsymbol{\zeta}_L\right)\cos(2\phi_{\rho-}+8t_\perp x/v),\end{aligned}\tag{4.6}$$

where $g_{\rho\pm}=\frac{1}{2}(g_{\rho(0,0,0)}\pm g_{\rho(\pi,0,0)})$ and $g_{\sigma\pm}=\frac{1}{2}(g_{\sigma(0,0,0)}\pm g_{\sigma(\pi,0,0)})$. We note that the coupling constants $g_{\rho+}$ and $g_{\sigma+}$ are the same as defined in Eq. (3.17). From Eq. (4.6), one easily finds that the 6 Majorana fermions are not independent and are grouped into two triplets $\boldsymbol{\xi}$ and $\boldsymbol{\zeta}$. In the derivation of the above effective theory, we do not use any fixed point values of the coupling constants but simply have used symmetry constraints. This means that the structure of the theory maintains at finite energy scale. The physical meanings of the respective triplets becomes clear by noting the following relations. The total spin operator $\boldsymbol{S}$ [Eq. (2.13)] can be expressed in terms of the Majorana fermions in a local form as $\boldsymbol{S}=\int dx\,\boldsymbol{J}(x)$ with

$$\begin{aligned}J^x(x) &= -i\left(\xi^2_R\xi^3_R+\xi^2_L\xi^3_L\right),\\ J^y(x) &= -i\left(\xi^3_R\xi^1_R+\xi^3_L\xi^1_L\right),\\ J^z(x) &= -i\left(\xi^1_R\xi^2_R+\xi^1_L\xi^2_L\right).\end{aligned}\tag{4.7}$$

Similarly the total "charge" operator $\boldsymbol{Q}$ [Eq. (2.18)] can be expressed as $\boldsymbol{Q}=\int dx\,\boldsymbol{J}'(x)$ with

$$\begin{aligned}J'^x(x) &= -i\left(\xi^6_R\xi^4_R+\xi^6_L\xi^4_L\right),\\ J'^y(x) &= -i\left(\xi^4_R\xi^5_R+\xi^4_L\xi^5_L\right),\\ J'^z(x) &= -i\left(\xi^5_R\xi^6_R+\xi^5_L\xi^6_L\right),\end{aligned}\tag{4.8}$$

up to the Klein factor. Thus we find that the system has the "charge-triplet" excitations described by the $\boldsymbol{\zeta}_p=(\xi^4_p,\xi^5_p,\xi^6_p)$ Majorana fermions. The derivation of these relations is quite similar to that for the spin chains.[50] These current operators satisfy the SU(2) Kac-Moody algebra at level $k=2$.[45]

For the relevant interchain hopping, we also find high symmetry in the $\rho-$ mode. In this case, the terms $g_{\rho(0,0,\pi)}$ and $g_{\sigma(0,0,\pi)}$ in Eq. (4.6) can be neglected due to the presence of $8t_\perp x/v$ in the cosine potential and then the effective theory becomes SO(3)×SO(3)×U(1) symmetric, where the SO(3)×SO(3) is due to the formation of two Majorana triplets and the U(1) is due to the absence of the potential for the bosonic field $\phi_{\rho-}$. This picture is only valid for large interchain hopping, since the U(1) symmetry is retained dynamically while the SO(3)×SO(3) has a microscopic origin.

The U and $t_\perp$ dependences of the charge and spin gaps and of the crossover energy scale $t_\perp^{\rm eff}$ are shown in Fig. 8. The $U/t_\parallel$ dependence of the spin gap reproduce qualitatively the DMRG numerical results,[43] while our RG approach would overestimate the magnitude of the spin gap. As easily seen from Fig. 8, the energy scales of the charge and spin excitation gaps are different in the whole region of $U/t_\parallel$, which is contrast to the analysis based on the one-loop fixed-point behavior.[38]

Next we examine the fixed-point behavior of the present analysis. The fixed point values are

$$\begin{aligned}&g_{\rho(\pi,0,0)}=g_{\rho(\pi,0,\pi)}=-g_{\sigma(0,0,0)}=g_{\sigma(\pi,0,\pi)}=+g^*,\\ &g_{\rho(0,0,0)}=g_{\rho(0,0,\pi)}=g_{\sigma(0,0,\pi)}=g_{\sigma(\pi,0,0)}=0,\end{aligned}$$

where we find $g^*/(2\pi v)=2$ in the present case. This implies that the symmetry is dynamically extended *in the low-energy limit*. The effective theory in the low-energy limit has been analyzed in the one-loop RG scheme and is known to be described as the SO(8) Gross-Neveu model.[38] This effective theory can easily be reproduced from Eq. (4.6). To this end, we fermionize the $\phi^p_{\rho-}$ boson fields by introducing another set of Majorana fermions:

$$\frac{1}{\sqrt{2}}\left(\xi^8_R+i\xi^7_R\right)\equiv+\frac{\kappa_{\rho-}}{\sqrt{2\pi a}}\exp\left(i\,2\phi^R_{\rho-}\right),\tag{4.9a}$$

$$\frac{1}{\sqrt{2}}\left(\xi^8_L+i\xi^7_L\right)\equiv-\frac{\kappa_{\rho-}}{\sqrt{2\pi a}}\exp\left(i\,2\phi^L_{\rho-}\right),\tag{4.9b}$$

where $\kappa_{\rho-}$ is the Klein factor. These Majorana fields satisfy the same anticommutation relations as before. By using the Majorana fields ξ^n for $n=1,\cdots,8$ and by inserting the fixed-point values into Eq. (4.6), the fixed point Hamiltonian can be expressed as

$$\begin{aligned}\mathcal{H}^{\rm eff}_{\rm ladder} &= -i\frac{v}{2}\sum_{n=1}^{8}\left(\xi^n_R\partial_x\xi^n_R-\xi^n_L\partial_x\xi^n_L\right)\\ &+\frac{g^*}{4}\left(\sum_{n=1}^{8}\xi^n_R\,\xi^n_L\right)^2.\end{aligned}\tag{4.10}$$

which is called the SO(8) Gross-Neveu model.[38] Here we note that this symmetry enlargement occurs *in the low-energy limit*, where all the excitations can be regarded to have the same magnitude of the excitation gap. In the finite energy scale, however, this symmetry does not hold and has SO(3)×SO(3)×U(1) as seen in Eq. (4.6) for relevant interchain hopping.

Finally we examine the magnitude of the excitation gaps for the remaining modes, ξ^7 and ξ^8, and we show how the low-energy effective theory in the small interchain hopping $t_\perp\ll\Delta_\rho$ can be described and how the trivial limit of $t_\perp\to 0$ can be reproduced in this Majorana-fermion description. The

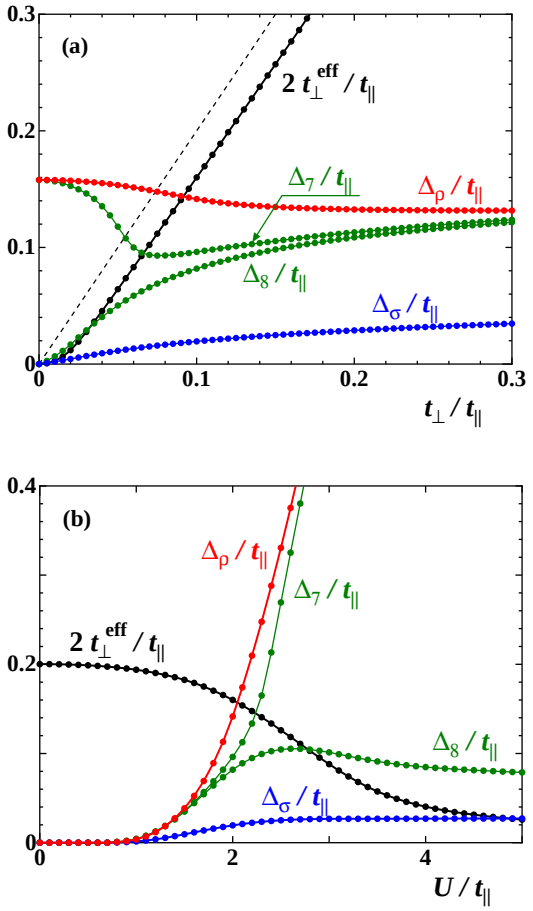

FIG. 8: (Color online) The excitation gaps, Δ_ρ (the charge gap), Δ_σ (the spin gap), Δ_7, Δ_8 (the gaps in the Majorana fermion ξ^7 and ξ^8, see text), and the characteristic energy scale $t_\perp^{\rm eff}$ for $N_\perp = 2$. (a) The $U/t_\parallel$ dependence with fixed $t_\perp/t_\parallel = 0.1$ and (b) the $t_\perp/t_\parallel$ dependence with fixed $U/t_\parallel = 2$. The dashed line represents the magnitude of the bare interchain hopping.

form of the Hamiltonian (4.6) is valid even in the small $t_\perp$ region, however, the physical picture in the $t_\perp \to 0$ limit is not so trivial. In terms of the Majorana fermions ξ^n ($n = 1, \cdots, 8$), the Hamiltonian (4.6) in the $t_\perp \to 0$ limit can be rewritten as $\mathcal{H}_{\rm eff}|_{t_\perp \to 0} = \mathcal{H}^c_{\rm eff} + \mathcal{H}^s_{\rm eff}$ with

$$\mathcal{H}^c_{\rm eff} = -i\frac{v}{2}\sum_{n=4,5,6,7}(\xi^n_R\partial_x\xi^n_R - \xi^n_L\partial_x\xi^n_L) + \frac{g_\rho}{2}\left(\xi^4_R\xi^4_L + \xi^5_R\xi^5_L + \xi^6_R\xi^6_L + \xi^7_R\xi^7_L\right)^2, \quad (4.11a)$$

$$\mathcal{H}^s_{\rm eff} = -i\frac{v}{2}\sum_{n=1,2,3,8}(\xi^n_R\partial_x\xi^n_R - \xi^n_L\partial_x\xi^n_L) - \frac{g_\sigma}{2}\left(\xi^1_R\xi^1_L + \xi^2_R\xi^2_L + \xi^3_R\xi^3_L - \xi^8_R\xi^8_L\right)^2, \quad (4.11b)$$

where g_ρ becomes relevant and g_σ becomes irrelevant. Here we adopt the notation $CnSm$ which denotes n massless *boson* modes in the charge sector and m massless *boson* modes in the spin sector.[20] If one assigns that the bosonic phase variables $\phi^p_{\rho\pm}$ and $\phi^p_{\sigma\pm}$ describe the "charge" and "spin" modes respectively, the $t_\perp \to 0$ limit may be interpreted as $C\frac{1}{2}S\frac{3}{2}$, where the gapless "spin" mode is described by the $\boldsymbol{\xi} = (\xi^1, \xi^2, \xi^3)$ fermion (the central charge is $c = \frac{3}{2}$) and the gapless "charge" mode is by the ξ^8 fermion (the central charge is $c = \frac{1}{2}$). The total central charge is consistent with that for two isolated Mott insulating chains $c = 2$, however, this picture is not correct obviously. The correct understanding in the $t_\perp \to 0$ limit is that the low-energy state is described by $C0S2$ where the Majorana fermions ξ^7 and ξ^8 should be regarded to describe the charge and spin degrees of freedom respectively. From this interpretation, we can expect that the magnitude of the gap in the Majorana fermions ξ^7 and ξ^8 shows nontrivial behavior as a function of $t_\perp$, since one (ξ^7) is gapped and the other (ξ^8) is gapless in the $t_\perp \to 0$, while these form the multiplet and are transformed into the U(1) bosonic field $\theta_{\rho-}$ in the large interchain hopping. In order to estimate the $t_\perp$ dependence of the gap in the Majorana fermions ξ^7 and ξ^8 of Eq. (4.6) from the numerical integration of the RG equations, we consider the following combination of the coupling

$$g_7 = \frac{1}{2}[g_{\rho(\pi,0,\pi)} + g_{\rho(0,0,\pi)}J(8t_\perp a/v) + g_{\sigma(\pi,0,\pi)} - g_{\sigma(0,0,\pi)}J(8t_\perp a/v)], \quad (4.12a)$$

$$g_8 = \frac{1}{2}[g_{\rho(\pi,0,\pi)} - g_{\rho(0,0,\pi)}J(8t_\perp a/v) + g_{\sigma(\pi,0,\pi)} + g_{\sigma(0,0,\pi)}J(8t_\perp a/v)], \quad (4.12b)$$

where $J(8t_\perp a/v)$ is a cutoff function satisfying $J(x) \approx 1$ for $x \ll 1$ and $J(x) \approx 0$ for $x \gg 1$. For relevant interchain hopping, we have $g_7 = g_8 = \frac{1}{2}(g_{\sigma(\pi,0,\pi)} + g_{\rho(\pi,0,\pi)})$, which would reflect the low-energy property of the $\theta_{\rho-}$ boson mode, and for $t_\perp \to 0$ we have $g_7 \to g_\rho$ and $g_8 \to g_\sigma$ reproducing the single-chain limit. The excitation gaps for these Majorana fermion are also shown in Fig. 8, where we have estimated by $\Delta_n = \Lambda e^{-l_n}$ with $G_n(l_n) = 0.7$ ($n = 7, 8$). The ground state of the present two-leg ladder system is known to be the D-Mott phase for arbitrary $t_\perp > 0$, however, as seen from Fig. 8(a), the crossover from the 1D-like Mott insulating state (having large charge gap and small spin gap) to the insulator of the ladder, which has SO(3)×SO(3)×U(1) symmetry, takes place at $t_\perp \approx \Delta_\rho|_{t_\perp=0}$ where and the excitation properties for the Majorana fermion ξ^7 and ξ^8 undergo considerable changes. By increasing $U/t_\parallel$ [Fig. 8(b)], the effective interchain hopping $t_\perp^{\rm eff}$ is suppressed extremely and the multiplet of the ξ^7 and ξ^8 splits into two isolated Majorana modes where the low energy excitations are described by the Majorana triplet $\boldsymbol{\xi} = (\xi^1, \xi^2, \xi^3)$ as a lowest-energy mode and by the Majorana singlet ξ^8 as a second-lowest-energy mode. This picture reproduces the low-energy properties of the Heisenberg spin ladder systems.[50]

The present estimations of the excitation gaps are also justified by noting that it reproduces the known quantum critical behavior obtained in the extended Hubbard model including the intersite Coulomb repulsion. The detailed estimation of the extended Hubbard model is given in the Appendix C.

V. CONCLUSIONS

In the present paper, we have derived the two-loop RG equations for the half-filled bipartite Q1D Hubbard model with the nonperturbative treatment of the interchain hopping, based on the conventional Kadanoff-Wilson approach. By considering finite number of 1D chains we have treated the transverse momentum $k_\perp$ as the patch index and have obtained the RG equations which can be extremely simplified reflecting the symmetry requirements of the Hubbard model. By solving these RG equations numerically, we have estimated the magnitude of the charge and spin gaps and clarified that the charge gap is suppressed due to the interchain hopping but is always finite even when the interchain hopping exceeds the magnitude of the charge gap. In order to justify the present approach, we have analyzed the RG scaling flows in the two-leg Hubbard case ($N_\perp = 2$) in detail based on the field-theoretical Majorana-fermion description and have clarified that the low-energy excitations have SO(3)×SO(3)×U(1) symmetry for large interchain hopping.

Acknowledgments

The author thanks C. Bourbonnais, Y. Suzumura, and Y. Fuseya for valuable discussions at early stage of the present work. The author also thanks T. Giamarchi, A. Furusaki, D.K. Campbell for useful discussions and comments. The numerical calculations were carried out in part on Altix3700 BX2 at YITP in Kyoto University.

APPENDIX A: CHARGE-SPIN DUALITY RELATION

In this section, we derive the pseudospin SU(2) relations (2.22) from the spin SU(2) relations (2.15) by using the "charge-spin duality" transformation. It is well known that the Hubbard Hamiltonian (2.1) is transformed to itself with $U \to -U$, under the particle-hole transformation for the spin down only,[51,52] i.e.,

$$c_{j,l,\uparrow} \leftrightarrow c_{j,l,\uparrow}, \quad c_{j,l,\downarrow} \leftrightarrow (-1)^{j+l} c^\dagger_{j,l,\downarrow}. \tag{A1}$$

Since the density operators are transformed as $(n_{j,l,\uparrow} + n_{j,l,\downarrow}) \leftrightarrow (n_{j,l,\uparrow} - n_{j,l,\downarrow})$ under this transformation, the charge and spin density operators are interchanged. In the Fourier space with the linearized dispersion, Eq. (A1) is rewritten as

$$c_{p,\uparrow}(\boldsymbol{k}) \leftrightarrow c_{p,\uparrow}(\boldsymbol{k}), \quad c_{p,\downarrow}(\boldsymbol{k}) \leftrightarrow c^\dagger_{p,\downarrow}((p\pi,\pi) - \boldsymbol{k}). \tag{A2}$$

By applying this transformation to the g-ology Hamiltonian (2.8), we find that the transformed Hamiltonian is given in the same form of Eq. (2.8), but the coupling constants are exchanged as

$$g_{1\perp(q,k_1,k_2)} \leftrightarrow -g_{3\perp(q,k_1,\pi-k_2)}, \tag{A3a}$$

$$g_{2\perp(q,k_1,k_2)} \leftrightarrow -g_{2\perp(\pi-q+k_1+k_2,k_1,k_2)}, \tag{A3b}$$

while $g_{\parallel(q,k_1,k_2)}$ and $g_{3\parallel(q,k_1,k_2)}$ are unchanged. In the spin part there are constraints (2.15) due to the spin-rotational SU(2) symmetry. By applying the duality relation (A3) to Eq. (2.15), we can derive the pseudospin SU(2) constraints (2.22).

APPENDIX B: FULL RG EQUATIONS FOR THE SPIN-ROTATIONAL INVARIANT CASE

In this section, the full two-loop RG equations are given in the case for the spin-rotational SU(2) symmetric case [Eq. (2.14)], without assuming the pseudospin SU(2) symmetry [Eq. (2.20)]. These RG equations are valid for the extended Hubbard model including additional spin-rotational symmetric interactions, e.g., intersite Coulomb repulsions.

The RG equation for the interchain hopping is given by

$$\frac{d}{dl}t_\perp = t_\perp - \frac{1}{4N_\perp^3}\sum_{q,k,k'} G^2_{\Sigma\mathrm{n}(q,k,k')}\, J_{0(q,k,k')} \cos k - \frac{1}{4N_\perp^3}\sum_{q,k,k'} G^2_{\Sigma\mathrm{u}(q,k,k')}\, J'_{0(q,k,k')} \cos k, \tag{B1}$$

where the second-order coupling constants contributing the self-energy corrections are put into forms:

$$G^2_{\Sigma\mathrm{n}(q,k,k')} \equiv \frac{1}{2}\Big[G^2_{\rho(q,k,k')} + 3\, G^2_{\sigma(q,k,k')}\Big], \tag{B2a}$$

$$G^2_{\Sigma\mathrm{u}(q,k,k')} \equiv \frac{1}{2}\Big[2\, G^2_{c(q,k,k')} + 2\, G^2_{c(\pi-q+k+k',k,k')} - 2\, G_{c(q,k,k')} G_{c(\pi-q+k+k',k,k')}\Big]. \tag{B2b}$$

The cutoff function $J_{0(q,k,k')}$ is given by Eq. (3.6a). In general, the cutoff function for the umklapp scattering contributions $J'_{0(q,k,k')}$ takes a different form from that for the normal scattering ones $J_{0(q,k,k')}$, however, if the system has the particle-hole symmetry, these become identical $J_{0(q,k,k')} = J'_{0(q,k,k')}$.

The RG equations for the coupling constants without the assumption of the spin-rotational SU(2) symmetry are given in symbolic form as

$$\frac{d}{dl}G_{\rho(q,k_1,k_2)} = \left[\frac{1}{2N_\perp}\sum_{k'}\Xi_{\rho 1(q,k_1,k_2,k')} + \frac{1}{8N_\perp^2}\sum_{q',k'}\Xi_{\rho 2(q,k_1,k_2,q',k')} + (k_1 \leftrightarrow k_2)\right] - \frac{1}{4N_\perp^2}\,G_{\rho(q,k_1,k_2)}\sum_{q',k'}\Xi_{3(q,k_1,k_2,q',k')}, \tag{B3a}$$

$$\frac{d}{dl}G_{\sigma(q,k_1,k_2)} = \left[\frac{1}{2N_\perp}\sum_{k'}\Xi_{\sigma 1(q,k_1,k_2,k')} + \frac{1}{8N_\perp^2}\sum_{q',k'}\Xi_{\sigma 2(q,k_1,k_2,q',k')} + (k_1 \leftrightarrow k_2)\right] - \frac{1}{4N_\perp^2}\,G_{\sigma(q,k_1,k_2)}\sum_{q',k'}\Xi_{3(q,k_1,k_2,q',k')}, \tag{B3b}$$

$$\frac{d}{dl}G_{c(q,k_1,k_2)} = \left[\frac{1}{2N_\perp}\sum_{k'}\Xi_{c1(q,k_1,k_2,k')} + \frac{1}{8N_\perp^2}\sum_{q',k'}\Xi_{c2(q,k_1,k_2,q',k')} + \Big((q,k_1,k_2)\to(-q,\pi-k_2,\pi-k_1)\Big)\right] - \frac{1}{4N_\perp^2}\,G_{c(q,k_1,k_2)}\sum_{q',k'}\Xi_{c3(q,k_1,k_2,q',k')}, \tag{B3c}$$

where $\Xi_{\nu 1}$ and $\Xi_{\nu 2}$ represent the one-loop Peierls/Cooper bubble contributions and the two-loop (third-order) vertex contributions, respectively, and Ξ_3 and Ξ_{c3} represent the two-loop (second-order) self-energy contributions. The respective terms are given explicitly in the following. The one-loop Peierls and Cooper bubble contributions are given by

$$\begin{aligned}\Xi_{\rho 1(q,k_1,k_2,k')} &= \frac{1}{2}\big[G_{\rho(q,k_1,k')}\,G_{\rho(q,k',k_2)} + 3G_{\sigma(q,k_1,k')}\,G_{\sigma(q,k',k_2)}\big]I_{(q,k',k_1,k_2)} \\ &\quad - \frac{1}{2}\big[G_{\rho(q-k_2+k',k_1,k')}\,G_{\rho(q-k_1+k',k',k_2)} + 3G_{\sigma(q-k_2+k',k_1,k')}\,G_{\sigma(q-k_1+k',k',k_2)}\big]I_{C(q-k_1-k_2,k',k_1,k_2)} \\ &\quad + 2\big[G_{c(q,k_1,k')}\,G_{c(q,k_2,k')} + G_{c(\pi-q+k_1+k',k_1,k')}\,G_{c(\pi+q-k_2-k',\pi-k',\pi-k_2)} \\ &\qquad - G_{c(q,k_1,k')}\,G_{c(\pi+q-k_2-k',\pi-k',\pi-k_2)}\big]I'_{(-q,\pi-k',\pi-k_1,\pi-k_2)},\end{aligned} \tag{B4a}$$

$$\begin{aligned}\Xi_{\sigma 1(q,k_1,k_2,k')} &= \big[G_{\rho(q,k_1,k')}\,G_{\sigma(q,k',k_2)} - G_{\sigma(q,k_1,k')}\,G_{\sigma(q,k',k_2)}\big]I_{(q,k',k_1,k_2)} \\ &\quad - \big[G_{\rho(q-k_2+k',k_1,k')} + G_{\sigma(q-k_2+k',k_1,k')}\big]G_{\sigma(q-k_1+k',k',k_2)}I_{C(q-k_1-k_2,k',k_1,k_2)} \\ &\quad - 2\big[G_{c(q,k_1,k')}\,G_{c(q,k_2,k')} - G_{c(q,k_1,k')}\,G_{c(\pi+q-k_2-k',\pi-k',\pi-k_2)}\big]I'_{(-q,\pi-k',\pi-k_1,\pi-k_2)},\end{aligned} \tag{B4b}$$

$$\begin{aligned}\Xi_{c1(q,k_1,k_2,k')} &= \big[G_{\rho(q,k_1,k')}G_{c(q,k',k_2)} - 3G_{\sigma(q,k_1,k')}\,G_{c(q,k',k_2)} + 2G_{\sigma(q,k_1,k')}\,G_{c(\pi-q+k'+k_2,k',k_2)}\big]I''_{(q,k',k_1,k_2)} \\ &\quad + \big[G_{\rho(\pi-q+k_1+k_2,k_1,k')}\,G_{c(q-k_1+k',k',k_2)} + G_{\sigma(\pi-q+k_1+k_2,k_1,k')}\,G_{c(q-k_1+k',k',k_2)}\big]I''_{(\pi-q+k_1+k_2,k',k_1,k_2)}.\end{aligned} \tag{B4c}$$

Due to the particle-hole symmetry of the present model on the bipartite lattice, the respective cutoff functions satisfy $I'_{(q,k',k_1,k_2)} = I''_{(q,k',k_1,k_2)} = I_{(q,k',k_1,k_2)}$, $I_{(-q,\pi-k',\pi-k_1,\pi-k_2)} = I_{(q,k',k_1,k_2)}$, and $I_{C(q-k_1-k_2,k',k_1,k_2)} =$

$I_{(\pi-q+k_1+k_2,k',k_1,k_2)}$, where $I_{(q,k',k_1,k_2)}$ is given in Eq. (3.1). The two-loop vertex contributions are given by

$$\begin{aligned}
\Xi_{\rho 2(q,k_1,k_2,q',k')} &= G_{\rho(q+q',k_1,k_2)}\big[G_{\rho(q-k_1+k',k',k'-q')}\,G_{\rho(q-k_2+k',k',k'-q')} \\
&\quad + 3G_{\sigma(q-k_1+k',k',k'-q')}\,G_{\sigma(q-k_2+k',k',k'-q')}\big]J_{2(q+k';k_1,k_2;k',k'-q')} \\
&\quad - 2G_{\rho(\pi-q-q'+k_1+k_2,k_1,k_2)}\big[G_{c(q-k_1+k',k',k'-q')}\,G_{c(q-k_2+k',k',k'-q')} \\
&\quad + G_{c(\pi-q-q'+k_1+k',k',k'-q')}\,G_{c(\pi-q-q'+k_2+k',k',k'-q')} \\
&\quad - G_{c(q-k_1+k',k',k'-q')}\,G_{c(\pi-q-q'+k_2+k',k',k'-q')}\big]J'_{2(q+k';k_1,k_2;k',k'-q')} \\
&\quad + G_{\rho(q-q',k_1-q',k_2-q')}\big[G_{\rho(k_1-k',k_1,k_1-q')}\,G_{\rho(k_2-k',k_2,k_2-q')} \\
&\quad + 3G_{\sigma(k_1-k',k_1,k_1-q')}\,G_{\sigma(k_2-k',k_2,k_2-q')}\big]J_{2(-k';-k_1,-k_2;\pi-k',\pi-k'+q')} \\
&\quad - 2G_{\rho(\pi+q+q'-k_1-k_2,\pi-k_1+q',\pi-k_2+q')}\big[G_{c(k_1-k',k_1,k_1-q')}\,G_{c(k_2-k',k_2,k_2-q')} \\
&\quad + G_{c(\pi-q'+k_1+k',k_1,k_1-q')}\,G_{c(\pi-q'+k_2+k',k_2,k_2-q')} \\
&\quad - G_{c(k_1-k',k_1,k_1-q')}\,G_{c(\pi-q'+k_2+k',k_2,k_2-q')}\big]J'_{2(-k';-k_1,-k_2;\pi-k',\pi-k'+q')}, \qquad \text{(B5a)} \\
\Xi_{\sigma 2(q,k_1,k_2,q',k')} &= G_{\sigma(q+q',k_1,k_2)}\big[G_{\rho(q-k_1+k',k',k'-q')}\,G_{\rho(q-k_2+k',k',k'-q')} \\
&\quad - G_{\sigma(q-k_1+k',k',k'-q')}\,G_{\sigma(q-k_2+k',k',k'-q')}\big]J_{2(q+k';k_1,k_2;k',k'-q')} \\
&\quad + 2G_{\sigma(\pi-q-q'+k_1+k_2,k_1,k_2)}\,G_{c(q-k_1+k',k',k'-q')}\,G_{c(\pi-q-q'+k_2+k',k',k'-q')}\,J'_{2(q+k';k_1,k_2;k',k'-q')} \\
&\quad + G_{\sigma(q-q',k_1-q',k_2-q')}\big[G_{\rho(k_1-k',k_1,k_1-q')}\,G_{\rho(k_2-k',k_2,k_2-q')} \\
&\quad - G_{\sigma(k_1-k',k_1,k_1-q')}\,G_{\sigma(k_2-k',k_2,k_2-q')}\big]J_{2(-k';-k_1,-k_2;\pi-k',\pi-k'+q')} \\
&\quad + 2G_{\sigma(\pi+q+q'-k_1-k_2,\pi-k_2+q',\pi-k_1+q')}\,G_{c(k_1-k',k_1,k_1-q')}\,G_{c(\pi-q'+k_2+k',k_2,k_2-q')} \\
&\quad \times J'_{2(-k';-k_1,-k_2;\pi-k',\pi-k'+q')}, \qquad \text{(B5b)} \\
\Xi_{c2(q,k_1,k_2,q',k')} &= \big[2G_{c(\pi-q-q'+k_1+k_2,k_1,k_2)}\,G_{\sigma(q-k_1+k',k',k'-q')}\,G_{\sigma(\pi-q-q'+k_2+k',k',k'-q')} \\
&\quad - G_{c(q+q',k_1,k_2)}\,G_{\rho(q-k_1+k',k',k'-q')}\,G_{\rho(\pi-q-q'+k_2+k',k',k'-q')} \\
&\quad + G_{c(q+q',k_1,k_2)}\,G_{\sigma(q-k_1+k',k',k'-q')}\,G_{\sigma(\pi-q-q'+k_2+k',k',k'-q')}\big]J''_{2(q+k';k_1,k_2;k',k'-q')} \\
&\quad + \big[2G_{c(\pi-q-q'+k_1+k_2,k_1-q',k_2-q')}\,G_{\sigma(k_1-k',k_1,k_1-q')}\,G_{\sigma(\pi+q'-k_2-k',\pi-k_2,\pi-k_2+q')} \\
&\quad - G_{c(q-q',k_1-q',k_2-q')}\,G_{\rho(k_1-k',k_1,k_1-q')}\,G_{\rho(\pi+q'-k_2-k',\pi-k_2,\pi-k_2+q')} \\
&\quad + G_{c(q-q',k_1-q',k_2-q')}\,G_{\sigma(k_1-k',k_1,k_1-q')}\,G_{\sigma(\pi+q'-k_2-k',\pi-k_2,\pi-k_2+q')}\big] \\
&\quad \times J''_{2(-k';-k_1,-k_2;\pi-k',\pi-k'+q')}, \qquad \text{(B5c)}
\end{aligned}$$

and the two-loop self-energy contributions are given by

$$\begin{aligned}
\Xi_{3(q,k_1,k_2,q',k')} &= G^2_{\Sigma\mathrm{n}(q',k_1,k')}\,J_{1(q',k_1,k')} + G^2_{\Sigma\mathrm{u}(q',k_1,k')}\,J'_{1(q',k_1,k')} \\
&\quad + G^2_{\Sigma\mathrm{n}(q',k_2,k')}\,J_{1(q',k_2,k')} + G^2_{\Sigma\mathrm{u}(q',k_2,k')}\,J'_{1(q',k_2,k')} \\
&\quad + G^2_{\Sigma\mathrm{n}(q',-k_1+q,k')}\,J_{1(q',-k_1+q,k')} + G^2_{\Sigma\mathrm{u}(q',-k_1+q,k')}\,J'_{1(q',-k_1+q,k')} \\
&\quad + G^2_{\Sigma\mathrm{n}(q',-k_2+q,k')}\,J_{1(q',-k_2+q,k')} + G^2_{\Sigma\mathrm{u}(q',-k_2+q,k')}\,J'_{1(q',-k_2+q,k')}, \qquad \text{(B6a)} \\
\Xi_{c3(q,k_1,k_2,q',k')} &= G^2_{\Sigma\mathrm{n}(q',k_1,k')}\,J_{1(q',k_1,k')} + G^2_{\Sigma\mathrm{u}(q',k_1,k')}\,J'_{1(q',k_1,k')} \\
&\quad + G^2_{\Sigma\mathrm{n}(q',\pi-k_2,k')}\,J_{1(q',\pi-k_2,k')} + G^2_{\Sigma\mathrm{u}(q',\pi-k_2,k')}\,J'_{1(q',\pi-k_2,k')} \\
&\quad + G^2_{\Sigma\mathrm{n}(q',-k_1+q,k')}\,J_{1(q',-k_1+q,k')} + G^2_{\Sigma\mathrm{u}(q',-k_1+q,k')}\,J'_{1(q',-k_1+q,k')} \\
&\quad + G^2_{\Sigma\mathrm{n}(q',\pi+k_2-q,k')}\,J_{1(q',\pi+k_2-q,k')} + G^2_{\Sigma\mathrm{u}(q',\pi+k_2-q,k')}\,J'_{1(q',\pi+k_2-q,k')}. \qquad \text{(B6b)}
\end{aligned}$$

The cutoff functions J_1 and J'_1 (J_2, J'_2, and J''_2) depend on the lattice geometry of the model and take different forms in general. However, in the present bipartite model, the respective cutoff functions satisfy $J'_{1(q,k,k')} = J_{1(q,k,k')}$, $J'_{2(q;k_1,k_2;k',k'')} = J''_{2(q;k_1,k_2;k',k'')} = J_{2(q;k_1,k_2;k',k'')}$. We also obtain $J_{1(-q,\pi-k_1,\pi-k_2)} = J_{1(q,k_1,k_2)}$ and $J_{2(-k';-k_1,-k_2;\pi-k',\pi-k'+q')} = J_{2(k';k_1,k_2;k',k'-q')}$ for the particle-hole symmetric case.

If the interaction is on-site one only, the system has the pseudospin SU(2) symmetry, where Eq. (2.22) is satisfied. By using Eq. (2.22), the coupling constant $G^2_{\Sigma(q,k,k')} = G^2_{\Sigma\mathrm{n}(q,k,k')} + G^2_{\Sigma\mathrm{u}(q,k,k')}$ can be rewritten in terms of G_ρ and

G_σ and reproduces Eq. (3.14). Then the RG equation for the interchain hopping [Eq. (B1)] leads Eq. (3.9) and those for the coupling constants [Eqs. (B3a) and (B3b)] lead Eq. (3.13). The explicit RG equations for the umklapp scattering [Eq. (B3c)] can be suppressed due to the pseudospin SU(2) symmetry [Eq. (2.22)].

APPENDIX C: EXTENDED TWO-LEG LADDER MODEL: CHECK OF QUANTUM CRITICAL BEHAVIOR

In Sec. III, we have estimated the magnitudes of charge and spin excitation gaps by using Eq. (3.18). If the charge and spin modes of the system are decoupled, such as in the single chain case, this method trivially works since the coupling constants representing respective modes are decoupled. However in the present $N_\perp$-chain system where the charge and spin degrees of freedom coupled with each other, one may consider that the present analysis does not work since the RG approach may break down at a energy scale corresponding to the largest excitation gap. In order to justify the present estimation of excitation gaps, we have considered the two-leg ladder model ($N_\perp = 2$) which is a minimal model with the spin and charge modes coupled. As already mentioned in Sec. IV, the U dependence of the spin gap [Fig. 8 (b)] shows similar behavior to the DMRG results[43]. In this section, we reconsider the two-leg ladder systems and we show another evidence which supports strongly the validity of the present estimation of excitation gaps.

We consider a toy model including an additional interaction V' which denotes the next-nearest-neighbor Coulomb repulsion. The spin mode in this model is known to exhibit quantum critical behavior within a nontrivial universality class. The purpose of the present section is to check whether the present method reproduces correct behavior of the quantum critical point (QCP). The Hamiltonian of this toy model is given by

$$\begin{aligned} H' &= -t_\parallel \sum_{j,l,s} \left(c^\dagger_{j,1,s} c_{j+1,1,s} + c^\dagger_{j,2,s} c_{j+1,2,s} + \text{H.c.} \right) \\ &\quad - 2t_\perp \sum_{j,s} \left(c^\dagger_{j,1,s} c_{j,2,s} + \text{H.c.} \right) \\ &\quad + U \sum_j \left(n_{j,1,\uparrow} n_{j,1,\downarrow} + n_{j,2,\uparrow} n_{j,2,\downarrow} \right) \\ &\quad + V' \sum_j \left(n_{j,1} n_{j+1,2} + n_{j,2} n_{j+1,1} \right). \end{aligned} \tag{C1}$$

The notations are the same as in Eq. (2.1). This extended two-leg ladder model is examined by the field-theoretical method[40]. For small V', the rung-singlet (or D-Mott) state is realized where the ground state is unique. By increasing V', this rung-singlet state changes into a spin-Peierls (or PDW) state (see Fig. 9 of Ref. 40) where the ground state has two-fold degeneracy and breaks translational invariance along the chain direction. From the field-theoretical approach, the quantum critical behavior is confirmed on the transition point between the rung-singlet state and the spin-Peierls state. On this

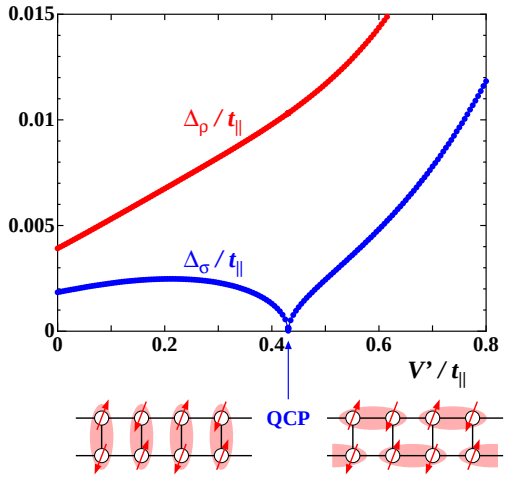

FIG. 9: (Color online) The $V'/t_\parallel$ dependences of the charge gap Δ_ρ and the spin gap Δ_σ, for the extended two-leg ladder model ($N_\perp = 2$) with $U/t_\parallel = 1$ and $t_\perp/t_\parallel = 0.5$.

QCP, the spin gap collapses and the effective theory for low-energy states is known to be described by the $c = 3/2$ conformal field theory where c is the central charge.

This extended Hubbard model can also be analyzed in the present framework of the two-loop RG, where the only differences from the analysis in Sec. III are that (i) the g-ology coupling constants in Eq. (2.8) have explicit momentum dependence and (ii) the pseudospin SU(2) [Eq. (2.22)] is not retained due to the presence of the additional interaction. The RG equations in this generalized case are given in the Appendix B. The estimated charge and spin gaps as a function of $V'/t_\parallel$ is shown in Fig. 9. We find that the present approach reproduces the critical behavior since the spin gap becomes small around the QCP and collapses just on the QCP. The critical value of V' is consistent with Fig. 9 in Ref. 40. The RG scaling flows on the QCP show that the coupling $G_{\rho+}$ reaches of the order unity for $l > l_{\rho+}$, however, the coupling $|G_{\sigma+}|$ remains small and becomes irrelevant $G_{\sigma+}(\infty) = 0$. Such scaling behavior is the same as expected from the field-theoretical approach,[40] and thus the present results can be justified even for spin-charge coupled systems.

From the technical point of view, we discuss the reason why the present analysis works even for spin-charge coupled systems. If one of the coupling constants reaches of the order unity in the scaling flow, the RG method breaks down where it can be understood that the corresponding mode has an excitation gap. In order to analyze the lower-energy properties further, the gapped mode should be traced out and one should derive the effective low-energy theory for remaining modes. Then one can apply the RG method to it again. In this context, the quantum critical behavior was confirmed in Refs. 40 and 41. As for the two-leg ladder systems, we find that this tracing-out procedure almost corresponds to the replacement of the relevant coupling constants to unity. On the other hand, in the scaling flow of the present two-loop RG, the coupling constants remain finite even for the relevant ones (see Fig. 6). Thus one can consider that such trancing-out procedure of the

gapped mode is performed automatically in the present two-loop RG approach. The minor differences between these two approaches do not affect the numerical results. Thus we find that the present approach to estimate the different energy gaps works even for spin-charge coupled systems.

Finally we note that the procedure of the derivation of the effective theory is not straightforward and restricted to the $N_\perp = 2$ case only. In the present estimation based on the two-loop RG, there is no need to derive such low-energy effective theory explicitly and thus this fact is the reason why it is easy to extend the analysis to the large number of chains systems.

[1] C. Bourbonnais, B. Guay, and R. Wortis, in *Theoretical Methods for Strongly Correlated Electrons* edited by D. Sénéchal, A.M. Tremblay, and C. Bourbonnais (Springer, New York, 2003), p. 77.

[2] V.J. Emery, in *Highly Conducting One-Dimensional Solids*, edited by J. Devreese, R. Evrard, and V. van Doren (Plenum, New York, 1979), p. 247.

[3] J. Sólyom, Adv. Phys. **28**, 201 (1979).

[4] C. Bourbonnais and L.G. Caron, Int. J. Mod. Phys. B **5**, 1033 (1991).

[5] T. Giamarchi, *Quantum Physics in One Dimension* (Oxford University Press, 2004).

[6] R. Shankar, Rev. Mod. Phys. **66**, 129 (1994).

[7] N. Furukawa, T.M. Rice, and M. Salmhofer, Phys. Rev. Lett. **81**, 3195 (1998), and references therein.

[8] D. Zanchi and H.J. Schulz, Europhys. Lett. **44**, 235 (1998); Phys. Rev. B **61**, 13609 (2000).

[9] M. Salmhofer, Commun. Math. Phys. **194**, 249 (1998).

[10] C.J. Halboth and W. Metzner, Phys. Rev. B **61**, 7364 (2000).

[11] C. Honerkamp, M. Salmhofer, N. Furukawa, and T.M. Rice, Phys. Rev. B **63**, 035109 (2001); M. Salmhofer and C. Honerkamp, Prog. Theor. Phys. **105**, 1 (2001); C. Honerkamp and M. Salmhofer, Phys. Rev. B **64**, 184516 (2001).

[12] D. Zanchi, Europhys. Lett. **55**, 376 (2001).

[13] C. Honerkamp and M. Salmhofer, Phys. Rev. B **67**, 174504 (2003).

[14] A.A. Katanin and A.P. Kampf, Phys. Rev. Lett. **93**, 106406 (2004).

[15] D. Rohe and W. Metzner, Phys. Rev. B **71**, 115116 (2005); W. Metzner, J. Reiss, and D. Rohe, Phys. Stat. Sol. B **243**, 46 (2006).

[16] J. Kishine and K. Yonemitsu, Phys. Rev. B **59**, 14823 (1999).

[17] H. Freire, E. Correa, and A. Ferraz, Phys. Rev. B **71**, 165113 (2005).

[18] For a review, C. Bourbonnais and D. Jérome, in *Advances in Synthetic Metals, Twenty Years of Progress in Science and Technology*, edited by P. Bernier, S. Lefrant, and G. Bidan (Elsevier, New York, 1999), p. 206.

[19] J. Kishine and K. Yonemitsu, J. Phys. Soc. Jpn. **67**, 2590 (1998); **68**, 2790 (1999).

[20] H.H. Lin, L. Balents, and M.P.A. Fisher, Phys. Rev. B **56**, 6569 (1997).

[21] R. Duprat and C. Bourbonnais, Eur. Phys. J. B **21**, 219 (2001).

[22] C. Bourbonnais and R. Duprat, J. Phys. IV France **114**, 3 (2004).

[23] Y. Fuseya and Y. Suzumura, J. Phys. Soc. Jpn. **74**, 1263 (2005).

[24] N. Dupuis, C. Bourbonnais, and J.C. Nickel, cond-mat/0510544; J.C. Nickel, R. Duprat, C. Bourbonnais, and N. Dupuis, Phys. Rev. B **73**, 165126 (2006).

[25] Y. Fuseya, M. Tsuchiizu, Y. Suzumura, and C. Bourbonnais, preprint.

[26] S. Dusuel and B. Douçot, Phys. Rev. B **67**, 205111 (2003).

[27] S. Biermann, A. Georges, A. Lichtenstein, and T. Giamarchi, Phys. Rev. Lett. **87**, 276405 (2001).

[28] S. Biermann, A. Georges, T. Giamarchi, and A. Lichtenstein, in *Strongly Correlated Fermions and Bosons in Low-Dimensional Disordered Systems*, edited by I.V. Lerner, B.L. Althsuler, V.I. Fal'ko, and T. Giamarchi (Kluwer Academic Publishers, Netherlands, 2002), p. 81.

[29] T. Giamarchi, S. Biermann, A. Georges, and A. Lichtenstein, J. Phys. IV France **114**, 23 (2004).

[30] C. Berthod, T. Giamarchi, S. Biermann, and A. Georges, cond-mat/0602304.

[31] F.H.L. Essler and A.M. Tsvelik, Phys. Rev. B **65**, 115117 (2002).

[32] For a review, E. Dagotto and T.M. Rice, Science **271**, 618 (1996), and references therein.

[33] M. Fabrizio, Phys. Rev. B **48**, 15838 (1993).

[34] A.A. Nersesyan, A. Luther, and F.V. Kusmartsev, Phys. Lett. A **176**, 363 (1993).

[35] D.V. Khveshchenko and T.M. Rice, Phys. Rev. B **50**, 252 (1994).

[36] H.J. Schulz, Phys. Rev. B **53**, R2959 (1996); in *Correlated Fermions and Transport in Mesoscopic Systems*, edited by T. Martin, G. Montambaux, and T. Trân Thanh Vân (Editions Frontières, Gif-sur-Yvette, France, 1996), p. 81.

[37] L. Balents and M.P.A. Fisher, Phys. Rev. B **53**, 12133 (1996).

[38] H.H. Lin, L. Balents, and M.P.A. Fisher, Phys. Rev. B **58**, 1794 (1998).

[39] M. Tsuchiizu and Y. Suzumura, Phys. Rev. B **59**, 12326 (1999).

[40] M. Tsuchiizu and A. Furusaki, Phys. Rev. B **66**, 245106 (2002).

[41] C. Wu, W.V. Liu, and E. Fradkin, Phys. Rev. B **68**, 115104 (2003).

[42] M. Tsuchiizu and Y. Suzumura, Phys. Rev. B **72**, 075121 (2005).

[43] R.M. Noack, S.R. White, and D.J. Scalapino, Phys. Rev. Lett. **73**, 882 (1994); Physica C **270**, 281 (1996).

[44] Z. Weihong, J. Oitmaa, C.J. Hamer, and R.J. Bursill, J. Phys.: Condens. Matter **13**, 433 (2001).

[45] A.O. Gogolin, A.A. Nersesyan and A.M. Tsvelik, *Bosonization and Strongly Correlated Systems* (Cambridge University Press, Cambridge, 1998).

[46] M. Tsuchiizu and A. Furusaki, Phys. Rev. Lett. **88**, 056402 (2002); Phys. Rev. B **69**, 035103 (2004).

[47] C.N. Yang, Phys. Rev. Lett. **63**, 2144 (1989); C.N. Yang and S.C. Zhang, Mod. Phys. Lett. **4**, 759 (1990); M. Pernici, Europhys. Lett. **12**, 75 (1990); S.C. Zhang, Phys. Rev. Lett. **65**, 120 (1990); H.J. Schulz, in *The Hubbard Model*, edited by D. Baeriswyl *et al.* (Plenum, New York, 1995), p. 89.

[48] A.A. Ovchinikov, Sov. Phys. JETP **30**, 1160 (1970).

[49] M. Tsuchiizu, Y. Suzumura, and C. Bourbonnais, unpublished.

[50] D.G. Shelton, A.A. Nersesyan, and A.M. Tsvelik, Phys. Rev. B **53**, 8521 (1996); A.A. Nersesyan and A.M. Tsvelik, Phys. Rev. Lett. **78**, 3939 (1997); A.M. Tsvelik, Phys. Rev. B **42**, 10499 (1990).

[51] H. Shiba, Prog. Theor. Phys. **48**, 2171 (1972);

[52] Y. Nagaoka, Prog. Theor. Phys. **52**, 1716 (1974).